1978, *Astron. Astrophys. Suppl.* **35**, 1-22.

COMPACT RADIO SOURCES IN THE GALACTIC CENTER REGION

D. DOWNES
Max-Planck-Institut für Radioastronomie, Bonn, Federal Republic of Germany
W.M. GOSS and U.J. SCHWARZ
Kapteyn Astronomical Institute, University of Groningen, The Netherlands
J.G.A. WOUTERLOOT
Sterrewacht, Huygens Laboratorium, Leiden, The Netherlands

Received May 22, 1978

This paper presents data on 74 compact radio continuum sources in the galactic center region, detected at 5 GHz with the Westerbork Synthesis Radio Telescope, together with information on the associated extended components measured at 4.875 and 10.7 GHz with the Bonn 100-m telescope. With the exception of Sgr B2, the flux in the compact sources is only a small percentage of that in the extended components. There is an unusual concentration of compact sources near $\ell = 0.2°$, which in general do *not* coincide with the ridge of the well-known spur or arc component seen on single-dish maps. The component MD5 in Sgr B2 has a turn-over frequency ≥ 8 GHz, and is one of the densest HII regions in the Galaxy. We also call attention to a previously unrecognized shell source, G359.1–0.5, which may be a supernova remnant. Supplementary observations at Westerbork provide a limit of 10 Jy for the flux density of Sgr A West at 610 MHz, which confirms that the electron temperature of the HII region surrounding the galactic nucleus is not out of the ordinary.

Key words: Galactic center – compact HII regions – supernova remnants

1. INTRODUCTION

Radio interferometry of the galactic center region has been mainly limited to Sagittarius A and the H II and molecular cloud complex at Sgr B2. This paper reports on the extension of partial-synthesis observations to other radio continuum sources in the region, and lists the new detections of a large number of compact components.

1.1 Westerbork observations

Observations were made with the Westerbork Synthesis Radio Telescope (WSRT) between 1973 and 1976 at a frequency of 4.995 GHz. Most of the fields were observed with either 20 or 40 aerial spacings over the full interferometer baseline of 1440 m. Some of the more complicated fields, such as those near $\ell = 0.1°$ and 0.2°, were observed with 80 spacings from 36 to 1440 m, in steps of 18 m. Since the shortest spacing was 36 m, source structures $\geq 3'$ were heavily attenuated. Elliptical grating lobes occurred at intervals of $2.9' \times 6.0'$ $(\alpha \times \delta)$ from main-beam responses in the maps with 20 spacings, and at two and four times larger intervals for the maps with 40 and 80 spacings, respectively. All of the maps were "cleaned" with the procedure described by Högbom (1974) (for a discussion of the mathematical uniqueness of the cleaning procedure, see Schwarz 1978). The restored beam was typically $6'' \times 40''$ to half-power, and in some cases the data were smoothed to larger effective beamwidths. The Westerbork data from the field centered on Sgr B2 were combined with Owens Valley observations (Rogstad *et al.* 1974) in the same way as was previously done for Sgr A (Ekers *et al.* 1975). None of the Westerbork maps in the figures in this paper have been corrected for attenuation by the primary beam. The flux densities in the source list, however, are corrected values.

The positions of the fields observed are shown in figure 1, superimposed on the Bonn map at 4.875 GHz (Altenhoff *et al.* 1978). The approximate field of view, indicated by the diameter of the shaded circles in figure 1, was 10.8′, the primary beam of the 25-m Westerbork antennas at 5 GHz. Additional fields, somewhat farther from the galactic equator, have been mapped at Westerbork at 1.4 GHz, and will be described in a separate paper (Wouterloot 1978).

Max-Planck-Gesellschaft zur Förderung der Wissenschaften e.V.
M.P.I. f. Radioastronomie, Bonn
Sonderdruck Nr. 304, Ser. A

1.2 Bonn observations

Information on the more extended continuum radiation in the vicinity of the compact components seen at Westerbork is provided by Bonn observations at 4.875 and 10.7 GHz. The data at 4.875 GHz are from the survey of the galactic plane by Altenhoff *et al.* (1978), with a half-power beamwidth of 2.6′. The data at 10.7 GHz were taken with the 100-m telescope with a cooled parametric amplifier of system temperature 100 K and IF bandwidth 50 MHz. The aperture efficiency was 0.40 and the beamwidth 1.3′. The 10.7 GHz data on Sgr B2 were taken at Bonn in collaboration with Dr. F.F. Gardner, CSIRO, Sydney. Preliminary versions of some of the 10.7 GHz maps were described by Downes (1974).

2. TABLE OF SOURCES

The sources are listed in table 1, in order of galactic longitude, with the following data.

Column 1: the number by which the compact sources are identified in the figures;

Columns 2 and 3: galactic coordinates of the compact sources;

Columns 4 and 5: right ascension and declination of the compact components for epoch 1950.0. The positions were measured from Westerbork maps, and the uncertainties are typically 0.1^s in R.A., and 5″ in Dec.

Column 6: flux density of the compact sources measured at Westerbork, corrected for attenuation by the primary beam pattern. The uncertainty is typically ± 0.01 Jy.

Column 7: deconvolved width of the compact sources to half-power, in R.A. We assumed that the sources were gaussians, and corrected the observed widths for broadening by the 6″ beam. We only list a width in R.A., since the Westerbork observations have relatively poor resolution in declination.

Columns 8 and 9: right ascension and declination (1950.0) of the extended components. The coordinates were taken from 10.7 GHz maps when available, otherwise from the 4.875 GHz survey. Uncertainties are typically $\pm 1^s$ in R.A. and $\pm 15''$ in Dec.;

Columns 10 and 11: integrated flux densities, estimated with a gaussian approximation, at 4.875 and 10.7 GHz for the extended components. Uncertainties are about $\pm 20\%$;

Column 12: deconvolved half-power width of the extended components. The value is the geometric mean of the minor and major axes, corrected for gaussian beams of 2.6′ at 4.875 GHz and 1.3′ at 10.7 GHz. When the results were discrepant, we listed only the diameters derived at 10.7 GHz;

Column 13: remarks or source identifications. Among the sources in Sgr B2, we give the previous designations in the list of Martin and Downes (1972). For completeness, we also include data on the components in Sgr A, from Ekers *et al.* (1975) and Kellermann *et al.* (1977). The transient radio source in Sgr A has not been observed at Westerbork, but we list the position measured at 0.96 GHz by Davies *et al.* (1976).

We do not tabulate all of the extended components in the galactic center region, but only those in the immediate vicinity of the compact sources. For a more complete list of the extended components, see the table of sources by Altenhoff *et al.* (1978). The sources listed in the present paper are plotted in figure 2, which is a composite of the Bonn maps at 4.875 and 10.7 GHz. The black dots denote the positions of the compact sources observed with interferometers, and the numbers in parentheses next to the dots are the identification numbers from column (1) in the source list. The diameters of the black circles are the half-power widths in R.A. (or their upper limits), measured at Westerbork.

3. COMMENTS ON SELECTED SOURCES

3.1 **G359.4–0.1**

The nature of G359.4–0.1 has been elusive for some time, because of the difficulty of separating the radio source from the background ridge. There are five distinct radio components:

a) a core source of diameter 26″ and flux density 1.3 Jy at 5 GHz (Westerbork map; figure 3, right);

b) an envelope of diameter 1.3′ about the core source, which is visible as the more extended contours on the Westerbork map, as the strong peak on the Bonn map at 10.7 GHz (figure 3, left). The total flux in the 10.7 GHz peak is 4.2 Jy, including the core source, so that ~ 3 Jy is probably in the 1.3′ envelope alone;

c) a halo of diameter $5' \times 3'$ ($\ell \times b$), which is the source seen on maps of lower resolution (beams $>3'$);

d) a tail of emission to the southwest, parallel to the galactic plane, which can be seen on the maps at 10.7 GHz (figure 3) and at 15.5 GHz (Kapitzky and Dent 1974);

e) wings or spurs of emission perpendicular to the galactic plane, which show up on the maps at 4.875 GHz (Altenhoff *et al.* 1978) and 0.408 GHz (Little 1974).

Components d) and e) contribute to fluxes measured previously with beams $>5'$. Figure 4 shows the flux densities of components a)–c) only, derived from maps with beams $<5'$. The overall spectrum is flat, at a level of ~ 10 Jy for the sum of the three components.

Recombination lines from G359.4–0.1

Since initial searches for a radio recombination line in G359.4–0.1 were unsuccessful (Reifenstein *et al.* 1970, Whiteoak and Gardner 1973), the source was considered a possible supernova remnant. Recent observations with long integration times reveal at least three lines, at -4, -60 and -130 km s^{-1} (see Pankonin and Downes 1976, for a review of recombination-line observations toward this source). The lines at -4 and -130 km s^{-1} are prominent at frequencies <2 GHz, as would be expected for extended, tenuous ($N_e \sim 20$ cm^{-3}) gas. The line at -60 km s^{-1} is more spatially localized. It does not appear, for example, in the H166α data of Kesteven and Pedlar (1977) taken with a 12′ beam. However, with a 2.6′ beam centered on the continuum peak the H110α line antenna temperature at -60 km s^{-1} is 0.2 K (Downes *et al.* 1978). This is about the value expected from a normal HII region with the observed continuum $T_a = 6.4$ K (after subtraction of the galactic ridge).

The line was probably not found by previous observers because the source consists of a superposition of several continuum components of different sizes and different radial velocities. Observers with large beams would therefore not see the usual line-to-continuum ratio characteristic of a single HII region. With an 8′ beam at 1.4 GHz, for example, the line components cover a velocity range ΔV of ~ 200 km s^{-1} (Pankonin and Downes 1976). The T_L/T_C ratio measured with beams $\geq 6'$ would thus be a factor of ~ 6 lower than the usual value for spiral-arm HII regions, which typically have $\Delta V \sim 30$ km s^{-1}.

Other data on G359.4–0.1

G359.4–0.1 is a far infrared source (Hoffmann *et al.* 1971, Alvarez *et al.* 1974, Gatley *et al.* 1978), with no strong central condensation. Molecular clouds with large negative velocities are seen in absorption against G359.4–0.1 in HI, OH and H_2CO (Kazès and Aubry 1973, Robinson and McGee 1970, Cohen and Few 1976, Scoville *et al.* 1972). Because of this absorption, and the recombination-line velocity of -60 km s^{-1}, the source must lie in the galactic center region. G359.4–0.1 thus appears to be a normal, flat-spectrum HII region, located in the nuclear disk.

3.2 Sources from $\ell = 0.0°$ to $0.2°$

Figure 5 shows the unusual concentration of compact sources in this region. The sources seen at Westerbork (solid contours, with shading) are superimposed on the Bonn 10.7 GHz contours (dashed lines).

It is difficult to interpret this remarkable collection of compact sources. The compact components near $\sim 17^h42^m30^s$, $-28°50'$ ($\ell \sim 0.1°$, $b \sim +0.05°$) are probably HII regions, embedded in the more extended radiation seen at 10.7 GHz. The extended gas at this location is certainly thermal, since it emits strongly in radio recombination lines (Pauls *et al.* 1976, Gardner and Whiteoak 1977). Furthermore, the extended source at

10.7 GHz which is labeled G0.18–0.04 in figure 6, has a strong recombination line and appears to be an HII region in the nuclear disk (Pauls *et al.* 1976, Gardner and Whiteoak 1977; the former authors report a maximum in line emission on the continuum peak, at -26 km s^{-1}; the latter authors have the line maximum somewhat to the north, at $+15$ km s^{-1}).

The *compact* sources near the extended spur or arc at $\ell = 0.2°$, however, are more puzzling. These sources are not especially concentrated to the peaks of the 10.7 GHz radiation, as is the case with compact components in Sgr B2, for instance. Moreover, they do *not* lie along the ridge line of the 10.7 GHz emission, perpendicular to the galactic plane, but rather along a curve, partially outside of 10.7 GHz spur.

One possibility is that all of the compact components shown in figures 5 and 6 are simply HII regions similar to most of the other sources discussed in this paper. However the 10.7 GHz peak at G0.16–0.15 (figure 6) appears to be nonthermal, with no radio recombination line (Pauls *et al.* 1976). We therefore suggest an alternative interpretation of the radio emission in this region, as follows.

The appearance of the spur or "arc" component, running perpendicular to the galactic plane on single-dish maps, may be partly coincidental. It might be caused by the blending together of an elongated nonthermal filament at 0.16–0.15 with an HII region at 0.18–0.04 (figure 6). The more relevant structure for understanding the region may be the curved line of compact sources, and the underlying extended radiation in the vicinity, delineated by contours 1, 2 and 3 in figure 6. Taken together, the compact sources and the weaker extended contours seem to lie in a ring or shell of diameter $\sim 12'$, the center of which may be the "hole" in the contours at $17^h43^m17^s$, $-28°53'30''$ (1950).

The arguments in favor of this interpretation are:

(i) The extended continuum emission at 0.16–0.15 shows no recombination lines (Pauls *et al.* 1976), and must therefore be nonthermal.

(ii) The region at 0.16–0.15 is strongest on the map of 0.408 GHz (Little 1974), whereas the HII region at 0.18–0.04 dominates the maps at higher frequencies. This is further evidence that the lower part of the spur or "arc" component must be nonthermal, with a slightly steeper spectral index than the upper part, at G0.18–0.04. The spectral index of G0.16–0.15 from 0.408 to 4.875 GHz is relatively flat however, $\alpha = -0.2$.

(iii) None of the far-infrared maps of the galactic center show much emission at the position of the proposed shell source (Alvarez *et al.* 1974, Jennings 1975, Fazio 1976). This is further evidence that the source is not an HII region, since one would otherwise expect to see far-infrared radiation from embedded and nearby dust. The maps at 100 and 540 μ by Gatley *et al.* (1977) and Hildebrand *et al.* (1978) do not cover the upper part of the arc. The small source G0.01–0.12 is present on the former map, however, and may thus be an HII region.

(iv) There is no strong emission of HCN at G0.16–0.15 (Fukui *et al.* 1977), and hence no evidence for the molecular clouds which are usually associated with galactic center HII regions.

(v) Both the distribution of the compact components and the curvature of the more extended contours on single-dish maps seem to define a shell source (figure 6).

The shell, if it really exists, may be a large, relatively old supernova remnant in the nuclear disk or along the line of sight. The compact sources seen at Westerbork would then resemble the filaments or knots that appear on interferometer maps of SNRs like IC443, the Cygnus Loop, Tycho or S147. The nonthermal ridge at G0.16–0.15 may be a strong filament which does not happen to lie on the shell boundary; such deviations from a smooth spherical shell are common in old SNR like HB21 and the Cygnus Loop.

The total flux within the proposed shell is ~ 35 Jy at 10.7 GHz. If the spectral index is -0.2, as indicated by comparison with Little's map at 0.408 GHz, then the surface brightness-diameter relation (e.g., Clark and Caswell 1976) implies a distance of ~ 7 kpc. While this value is not too meaningful, it is at least consistent with the interpretation of a supernova remnant at about the distance of the nuclear disk.

We may also compare the source with another previously unrecognized shell in the direction of the galactic center region, G359.1–0.5. Except for its lower surface brightness, G359.1-0.5 is similar in shape and size to the shell which we are proposing at G0.2–0.2.

3.3 **A new shell source at G359.1–0.5**

Figure 7 shows a previously uncatalogued, nearly circular ring at 359.1–0.5, from the 4.875 GHz data of Altenhoff *et al.* (1978). It has probably not been noticed by earlier observers because its contours are blended with the radiation of the background ridge. The angular diameter of the object is 21′, nearly twice that of the proposed shell source at 0.2–0.2. Because of its large size and its galactic latitude, we suspect that G359.1–0.5 is an old supernova remnant lying along the line of sight to the galactic center, but not in the nuclear disk itself. At 4.875 GHz, the flux density of G359.1–0.5 is ~ 13 Jy. If the source is indeed a supernova remnant, with a typical spectral index of -0.5, then the surface brightness-diameter relation suggests a distance of ~ 6 kpc. The uncertainty is large, however.

3.4 **G0.5–0.6 and G0.56–0.85**

Figure 8 shows the Westerbork map of the group of sources near G0.5–0.6. Comparison with figure 2 indicates that the compact components are embedded in two extended HII regions, G0.489–0.668 and G0.572–0.628 (Altenhoff *et al.* 1978). The radio recombination lines from the latter HII region has a low LSR velocity (12 km s^{-1}) and a relatively normal width (17 km s^{-1}). Pauls and Mezger (1975) therefore concluded that the source was a foreground object, along the line of sight to the galactic center. The compact components seen at Westerbork are presumably the denser clumps within the extended HII gas.

G0.56–0.85

We include in figure 2 and table 1 two compact sources detected at 1.4 GHz by Miley (private communication), in the extended HII region G0.56–0.85. One of the compact components, 0.547–0.851, coincides within the errors ($\pm 5''$) with the position of the H_2O maser measured by Genzel and Downes (1977). Apart from Sgr B2, this is the only source in the galactic center direction in which an H_2O maser has been found. The HII region at this position can be seen on the Palomar prints, however (cf. Gardner and Whiteoak 1975), so G0.56–0.85 probably does not lie in the nuclear region, but is instead a foreground object like the sources at 0.5–0.6.

3.5 **Sgr B2**

Figure 9 shows the Bonn map at 10.7 GHz, and the map made from the combined data from Westerbork (this paper) and from Owens Valley (Rogstad *et al.* 1974). The synthesis map confirms the components originally found by Martin and Downes (1972), and adds a few new fainter ones.

Figure 10 gives the radio spectrum of various components in Sgr B2, derived from interferometer and single-dish measurements. As in many large HII regions, the spectrum of Sgr B2 below 1 GHz falls off less steeply than a Rayleigh-Jeans law, probably because of large-scale density gradients in the ionized gas. One of the stronger of the compact components, MD4, has a size of 11″ and a flat spectrum above 2.7 GHz, characteristic of optically thin plasma.

The high-density component in Sgr B2

The fringe amplitude measured for Sgr B2 with different radio interferometers increases strongly with frequency between 2.7 and 8 GHz (figure 11, lower). In contrast, the compact structure embedded in Sgr A West has a flat spectrum, since the interferometer fringe amplitudes are the same at different frequencies (figure 11, upper) (the flux of the radio point source in Sgr A increases slowly with frequency (Brown *et al.* 1978), but this increase is too small to be seen on the scale of figure 11).

In Sgr B2, most of the increase in the fringe amplitudes is due to component MD5. This component has a size of $\sim 7''$, and is optically thick at 2.7 GHz. At frequencies >8 GHz, the interferometer fringe amplitude of MD5 no longer rises (figure 11), indicating that the source has become optically thin. These

interferometer measurements >8 GHz provide the upper limits plotted in figure 10 for the flux of MD5. The source thus has a turn-over frequency at about 8 GHz, an emission measure of 8 10^7 cm^{-6} pc, an ionized mass of ~ 7 $M_\odot$, and an electron density of 1.5 10^4 cm^{-3}, which makes it one of the more dense HII regions in the Galaxy.

It therefore appears that the spectrum plotted by Thum *et al.* (1978) leads to serious overestimates of the flux of MD5 at 22 GHz, since those authors undoubtedly included a more extended component, as well as the compact sources MD3 and MD5 in their measurements. In fact, the source MD5 probably attains no greater a flux than had already been known since 1974 from the measurements of Balick and Sanders.

It is also fairly certain that this radio component does *not* account for the excess flux density of Sgr B2 at a wavelength of 3 mm (Hobbs *et al.* 1971, Righini *et al.* 1976). Figure 10 shows that the flux measured in a 1.3′ beam at 10.7 GHz (16 Jy; this paper) is practically the same as that measured with the same size beam at 85 GHz (21 Jy; Righini *et al.* 1976). An excess of 5 to 8 Jy in a 1.3′ beam at 85 GHz can be easily accounted for by the radiation from dust in Sgr B2, which has the familiar ν^3 spectrum in the millimeter region (figure 10).

3.6 G0.9+0.1 and G0.8+0.2

The Bonn and Westerbork maps of the area around G0.9+0.1 are given in figure 12. About half of the flux of the main peak at 10.7 GHz is contained in the compact components (72) and (73); the remainder comes from emission extended over $\sim 6'$ which is missing from the Westerbork map.

Although G0.9+0.1 has a flat spectrum (figure 13), no recombination line has ever been found (Reifenstein *et al.* 1970, Whiteoak and Gardner 1973, Pauls and Mezger 1975). Furthermore, no infrared sources have yet been reported at the position of the radio source.

Several of the galactic center molecular clouds appear in H_2CO absorption against G0.9+0.1 (Scoville *et al.* 1972, Whiteoak and Gardner 1974). The source must therefore lie in or beyond the nuclear disk. It appears to be either a flat-spectrum SNR like 3C58 or else an extragalactic source.

The weaker source G0.8+0.2 has a recombination line at 10 km s^{-1} (Downes *et al.* 1978) and appears to be an HII region. There is a strong absorption line at -24 km s^{-1} against this source, which is characteristic of some clouds seen toward the galactic center. The source may therefore also lie in or beyond the nuclear disk.

3.7 G1.1–0.1

The Bonn and Westerbork maps of this region are shown in figure 14, and the spectra of the various components are given in figure 15. The nonthermal source, G1.05–0.1, which is presumably a supernova remnant, is especially prominent on the map by Little (1974) at 0.408 GHz, and in lunar occulation observations (Swarup *et al.* 1974, Taylor 1968). The weak H109 α line (Pauls and Mezger 1975) implies that a small HII region is superimposed on the SNR.

The thermal source G1.1–0.1, which contains the compact component seen at Westerbork, is presumably in the nuclear disk, because of the strong H_2CO absorption of this source by galactic center molecular clouds with a wide range in velocity (Whiteoak and Gardner 1974, Kazès and Aubry 1973).

4. INTERPRETATION OF THE COMPACT SOURCES

Most of the compact sources reported here are probably galactic. The number of extragalactic sources with 5 GHz flux density ≥0.02 Jy, the minimum value in our source list, is 1.3 10^4 per steradian (Pauliny-Toth *et al.* 1978). For the 1.7 10^{-4} steradians covered in the 21 search fields marked in figure 1, only two extragalactic sources are expected, compared with an observed number of 74 compact sources.

Sources in the direction of the galactic center which may be supernova remnants are: G359.1–0.5, G0.2–0.2, G0.9+0.1, G1.05–0.1 and Sgr A East. With the exception of the compact sources near G0.2–0.2,

G0.9+0.1, and the radio point source in Sgr A West, most of the sources seen at Westerbork are probably compact HII regions embedded in more extended plasma of lower density. Typical parameters of the compact components are: emission measure 10^6 to 10^7 cm^{-6} pc, electron density 10^3 to 10^4 cm^{-3}, and ionized mass 5 to 30 $M_\odot$. For comparison, if the central region of the Orion Nebula were at the distance of the galactic center, it would have a flux density of 1.5 Jy, and an angular size of 15″, corresponding to some of the stronger components in the source list. NGC2024 would appear as a compact source of about 0.1 Jy, a typical source in our table, and Mon R2 would be a source of diameter 2″, and a flux density of 0.06 Jy, corresponding to the weaker sources in our list. Since a source like Mon R2 is excited by an O9 or B0 star (Beckwith *et al.* 1976, Downes *et al.* 1975), we conclude that we have detected nearly all of the optically thin HII regions in the galactic center which are excited by massive O stars, and that we are starting to see small HII regions, similar to Sharpless HII regions, which are excited by single stars of late O or early B type.

With the exception of Sgr B2, the galactic center HII regions are not like the massive young HII regions W49, W51 or W3, which have a large fraction of their radio flux in small-diameter components. A similar picture emerges from the infrared observations (Gatley *et al.* 1978). The galactic center region has no strong H_2O masers or Type I OH masers, except for those in Sgr B2. (As noted above, the OH and H_2O masers in G0.56–0.85 are probably not in the galactic center). This would seem to be further evidence that most of the compact radio components reported here are associated with late O and early B stars, rather than with very massive, recently-formed O stars.

Sagittarius A

The radio source Sagittarius A consists of two main components, referred to as Sgr A East and Sgr A West. The former component has a nonthermal spectrum and dominates the radio continuum at frequencies below 1 GHz. The latter component coincides in position with the maximum of the galactic center 2.2μ emission, and appears to be an HII region at the galactic nucleus. The spectrum of Sgr A West is flat between 1.4 and 5 GHz, but the source has not yet been definitely detected below 1.4 GHz.

The HII region Sgr A West is unusual because of the large line width of its radio recombination lines (Pauls *et al.* 1974), and its neon lines at 12.8μ (Wollman *et al.* 1976, 1977), and possibly because of the radio point source at its center. Rieke *et al.* (1978), however, list the ways in which Sgr A West resembles a normal galactic HII region like M17. To investigate this problem somewhat further, we have made new observations of Sgr A at 610 MHz, in order to get a limit on the low-frequency flux, and hence of the electron temperature, of Sgr A West.

5. ADDITIONAL OBSERVATIONS AT 610 MHz

The observations were made with 20 aerial spacings of the Westerbork telescope, over hour angles $\pm 2^h$ of transit. Grating responses occurred at intervals of 25′ in R.A. Ten db of extra attenuation were inserted to compensate for the strong signal at short spacings. Most of this signal comes from Sgr A East and the more extended, underlying continuum components, including the galactic ridge. A further correction was made for the non-linear response of the correlator, and these changes and corrections were checked against the calibration source 3C309. The data were made into a map, and the strong sidelobe responses were removed by the "clean" method described by Högbom (1974). The effective resolution was 35″ × 330″ (R.A. × Dec.).

The resulting map has information mainly in the direction of R.A., and shows the sources Sgr A and Sgr B2 (figure 16; prepared with the help of P. Shaver and R.D. Ekers, Kapteyn Astronomical Institute, Groningen). The position of Sgr A at 610 MHz is:

$$17^h42^m33.1^s \pm 0.5^s$$
$$-28°59'15'' \pm 10'', (1950.0)$$

which agrees with the positions obtained from measurements at lower frequencies (Maxwell and Taylor 1968, Thompson *et al.* 1969, Dulk and Slee 1974, Little 1974, Gopal-Krishna *et al.* 1972, 1976). It thus appears that even at 610 MHz, the position of the source has converged to its low-frequency limit, which we take to be centroid of Sgr A East.

The position which one derives for the peak of Sgr A East depends somewhat on the beam shape. Observations with resolution $\leq 40''$ in R.A. are dominated by a ridge or shell at $17^h42^m36^s$ (e.g. Sandqvist 1974, Ekers *et al.* 1975), while the observations with resolution $\geq 90''$ in R.A. give a position more consistent with the centroid of the brightness distribution of Sgr A East.

The total flux density which we measure for Sgr A at 610 MHz is 300 ± 50 Jy, and we estimate that ~ 50 Jy is probably in our fan beam from emission regions to the north of Sgr A (see figure 16), and should not be assigned to Sgr A itself. At 610 MHz, Sgr A has a halfwidth of $200''$ in R.A., with a slightly steeper slope on the eastern side than on the western.

In order to derive a limit for the flux density of Sgr A West, we used two models: (a) Sgr A East has an abrupt edge at $17^h42^m33^s$, where it joins with Sgr A West; (b) Sgr A East and West overlap smoothly, out to at least the 25-unit contour on the 5 GHz map by Ekers *et al.* (1975). We then calculated the effect on the observed map if Sgr A West had fluxes of 25, 15, 10 or 5 Jy at 610 MHz, with allowance for beam dilution. The net result in both models is that Sgr A West cannot have the same flux density, 25 Jy, at 610 MHz as it does at 1.4, 2.7 and 5 GHz. In fact, the models show that Sgr A West cannot be stronger than 10 Jy at 610 MHz, without distorting the map in figure 16.

This limit on the flux density of Sgr A West provides further confirmation that the source is an HII region, the other lines of evidence being:

(i) the flat spectrum above 1.4 GHz, characteristic of an optically thin thermal source;

(ii) the broad recombination line (Pauls *et al.* 1974), which has an integrated intensity consistent with the radio continuum temperature;

(iii) the neon II line at 12.8μ, which originates in ionized gas, and which has roughly the same extent as the radio source (Aitken *et al.* 1974, Wollman *et al.* 1976, 1977, Willner 1978);

(iv) the Brackett-gamma line, which originates over the central one parsec (angular size $20''$) of Sgr A West (Neugebauer *et al.* 1978);

(v) the self-consistent models of the radio and infrared continuum emission (Gatley *et al.* 1977, Rieke *et al.* 1978); the visual extinction from dust in the central region in these models is 6 mag, which in turn is consistent with the extinction derived from the color and silicate absorption in the compact, near infrared sources (Becklin *et al.* 1978).

(vi) the fact that the radio surface brightness of Sgr A West is far too low for the decrease in flux between 1.4 and 0.6 GHz to be the result of synchrotron self-absorption.

The flux limit at 610 MHz also gives a limit on the electron temperature of Sgr A West, from the Rayleigh-Jeans relation.

The temperature must be less than $1.6\ 10^4$ K. This temperature limit from direct measurement may be compared with the electron temperature of 6300 K derived by Pauls *et al.* from the broad recombination line which they observed in the direction of Sgr A. Since the beamwidth used by Pauls *et al.* was $2.6'$ and included both Sgr A East and West, as well as the more extended components underlying these sources, those authors assumed that the broad recombination line was coming partly from the underlying extended component, but mainly from Sgr A West, for which they used the continuum parameters observed at 5 GHz by Downes and Martin (1971).

The limit on the electron temperature suggests that the gas in Sgr A West is not collisionally ionized. The velocity and widths of the radio recombination line and the [Ne II] line, indicate that parts of Sgr A West have motions of ~ 100 km s^{-1}. However, the source is quite unlike other objects in the Galaxy which have motions of this order. In the Cygnus Loop and Vela Supernova remnants, for example, the 100 km s^{-1}

motion produces collisional ionization corresponding to temperatures of 10^6 K, and this ionized plasma is detected in soft X-rays. There is also gas in these remnants at 10^5 K, as well as filaments which have cooled by virtue of their higher density to 10^4 K. The fact that most of Sgr A West seems to have a rather ordinary electron temperature of $\sim 10^4$ K, implies that the source is ionized by ultraviolet radiation.

The limit on the flux of Sgr A West at 610 MHz also has implications for the location of the radio point source (Balick and Brown 1974). The spectrum of this source cuts off sharply between 1.6 and 0.4 GHz (Davies *et al.* 1976b). Its disappearance at 0.4 GHz is consistent with free-free absorption by Sgr A West, with the point source being actually located at the galactic nucleus.

ACKNOWLEDGEMENTS

We thank F.F. Gardner for collaborating on the 10.7 GHz map of Sgr B2, D. Rogstad and J. Whiteoak for providing their Owens Valley data, A. Baudry, M. Felli and B. Balick for the fringe visibilities measured at Hat Creek and Bordeaux, Stanford and NRAO, respectively. We thank G. Miley and J. Schmidt for unpublished data and P. Shaver and J. Bregman, Netherlands Foundation for Radio Astronomy, for data reduction and for help with the observations at 610 MHz. We are indebted to R.D. Ekers for useful discussions and to Professor J.H. Oort for his unflagging interest and encouragement in these observations. The Westerbork Synthesis Radio Telescope is operated by the Netherlands Foundation for Radio Astronomy with financial support of the Netherlands Organization for the Advancement of Pure Research (Z.W.O.).

REFERENCES

Aitken, D.K., Jones, B. and Penman, J.M.: 1974, *Monthly Notices Roy. Astron. Soc.* **169**, 35P.
Altenhoff, W.J., Downes, D., Pauls, T. and Schraml, J.: 1978, *Astron. Astrophys. Suppl.* (in press).
Alvarez, J.A., Furniss, I., Jennings, R.E., King, K.J. and Moorwood, A.F.M.: 1974, in A.F.M. Moorwood (ed.), *HII Regions and the Galactic Centre*, ESRO, Neuilly-sur-Seine, p. 69.
Ariskin, V.I., Berulis, I.I., Brezgunov, V.N., Dagkesamansky, R.D., Sorochenko, R.L. and Udaltsov, V.A.: 1973, *Radiofizika* **16**, 1334; 1975 *Radiophys. Quantum Electron.*, **16**, 1024.
Bagri, D.S.: 1975, Ph. D. Thesis, University of Bombay.
Balick, B. and Brown, R.L.: 1974, *Astrophys. J.* **194**, 265.
Balick, B. and Sanders, R.H.: 1974, *Astrophys. J.* **192**, 325.
Becklin, E.E., Matthews, K., Neugebauer, G. and Willner, S.P.: 1978, *Astrophys. J.* **220**, 831.
Beckwith, S., Evans, N.J., Becklin, E.E. and Neugebauer, G.: 1976, *Astrophys. J.* **208**, 390.
Berulis, I.I.: 1976, *Pisma Astron. Zh.* **2**, 23; 1976, *Soviet Astron. Lett.* **2**, 8.
Bieging, J.H.: 1976, *Astron. Astrophys.* **51**, 289.
Brown, R.L. and Broderick, J.J.: 1973, *Astrophys. J.* **181**, 125.
Brown, R.L., Lo, K.Y. and Johnston, K.J.: 1978, *Astrophys. J.* (in press).
Clark, D.H. and Caswell, J.L.: 1976, *Monthly Notices Roy. Astron. Soc.* **174**, 267.
Clegg, P.E. and Ade, P.A.R.: 1974, in A.F.M. Moorwood (ed.), *HII Regions and the Galactic Centre*, ESRO Neuilly-sur-Seine, p. 93.
Cohen, R.J. and Few, R.W.: 1976, *Monthly Notices Roy. Astron. Soc.*, **176**, 495.
Davies, R.D., Walsh, D., Browne, I.W.A., Edwards, M.R. and Noble, R.G.: 1976a, *Nature* **261**, 476.
Davies, R.J., Walsh, D. and Booth, R.S.: 1976b, *Monthly Notices Roy. Astron. Soc.* **177**, 319.
Downes, D.: 1974, in A.F.M. Moorwood (ed.), *HII Regions and the Galactic Centre*, ESRO, Neuilly-sur-Seine, p. 247.
Downes, D., Bieging, J., Wilson, T.L. and Wink, J.: 1978: *Astron. Astrophys.* in preparation.
Downes, D. and Martin, A.H.M.: 1971, *Nature* **233**, 112.
Downes, D. and Maxwell, A.: 1966, *Astrophys. J.* **146**, 653.
Downes, D., Maxwell, A. and Rinehart, R.: 1970, *Astrophys. J.* **161**, L123.
Downes, D., Winnberg, A., Goss, W.M. and Johansson, L.E.B.: 1975, *Astron. Astrophys.* **44**, 243.
Dulk, G.A. and Slee, O.B.: 1972, *Austral. J. Phys.* **25**, 429.
Dulk, G.A. and Slee, O.B.: 1974, *Nature* **248**, 33.
Ekers, R.D., Goss, W.M., Schwarz, U.J., Downes, D. and Rogstad, D.H.: 1975, *Astron. Astrophys.* **43**, 159.
Efanov, V.A., Moiseev, I.G. and Nesterov, N.S.: 1976, *Isvestia Krimsk. Astrophys. Obs.* **54**, 159.
Elias, J.H., Ennis, D.J., Gezari, D.Y., Hauser, M.G., Houck, J.R., Lo, K.Y., Matthews, K., Nadeau, D., Neugebauer, G., Werner, M.W. and Westbrook, W.E.: 1978, *Astrophys. J.* **220**, 25.
Eyles, C.J., Skinner, G.K., Willmore, A.P. and Rosenberg, F.D.: 1975, *Nature* **257**, 291.
Fazio, G.: 1976, private communication.

Felli, M., Tofani, G. and D'Addario, L.R.: 1974, *Astron. Astrophys.* **31**, 431.
Forster, J.R., Welch, W.J., Wright, M.C.H. and Baudry, A.: 1978, *Astrophys. J.* **221**, 137.
Fukui, Y., Iguchi, T., Kaifu, N., Chikada, Y., Morimoto, M., Nagane, K., Miyazawa, K. and Miyaji, T.: 1977, *Publ. Astron. Soc. Japan* **29**, 643.
Gardner, F.F. and Whiteoak, J.B.: 1975, *Monthly Notices Roy. Astron. Soc.* **171**, 29P.
Gardner, F.F. and Whiteoak, J.B.: 1977, *Proc. Astron. Soc. Australia* **3**, 150.
Gatley, I., Becklin, E.E., Werner, M.W. and Wynn-Williams, C.G.: 1977, *Astrophys. J.* **216**, 277.
Gatley, I., Becklin, E.E., Werner, M.W. and Harper, D.A.: 1978, *Astrophys. J.* **220**, 822.
Genzel, R., Downes, D. and Bieging, J.: 1976, *Monthly Notices Roy. Astron. Soc.* **177**, 101P.
Genzel, R. and Downes, D.: 1977, *Astron. Astrophys. Suppl.* **30**, 145.
Gopal-Krishna, Swarup, G., Sarma, N.V.G. and Joshi, M.N.: 1972, *Nature* **239**, 91.
Gopal-Krishna and Swarup, G.: 1976, *Astrophys. Letters* **17**, 45.
Goss, W.M., Knowles, S.H., Balister, M., Batchelor, R.A. and Wellington, K.J.: 1976, *Monthly Notices Roy. Astron. Soc.* **174**, 541.
Hildebrand, R.H., Whitcomb, S.E., Winston, R., Stiening, R.F., Harper, D.A. and Moseley, S.H.: 1978, *Astrophys. J.* **219**, L101.
Hobbs, R.W. and Johnston, K.J.: 1971, *Astrophys. J.* **163**, 299.
Hobbs, R.W., Modali, S.B. and Maran, S.P.: 1971, *Astrophys. J.* **165**, L87.
Hoffmann, W.F., Frederick, C.L. and Emery, R.J.: 1971, *Astrophys. J.* **164**, L23.
Högbom, J.A.: 1974, *Astron. Astrophys. Suppl.* **15**, 417.
Jennings, R.E.: 1975, in T.L. Wilson and D. Downes (eds.), *HII Regions and Related Topics*, Springer-Verlag, Berlin, p. 137.
Kapitzky, J.E. and Dent, W.A.: 1974, *Astrophys. J.* **188**, 27.
Kazès, I. and Aubry, D.: 1973, *Astron. Astrophys.* **22**, 413.
Kellermann, K.I., Shaffer, D.B., Clark, B.G. and Geldzahler, B.J.: 1977, *Astrophys. J.* **214**, L61.
Kesteven, M.J. and Pedlar, A.: 1977, *Monthly Notices Roy. Astron. Soc.* **180**, 731.
Little, A.G.: 1974, in F.J. Kerr and S.C. Simonson (eds.), Galactic Radio Astronomy, *IAU Symp. no. 60*, D. Reidel, Dordrecht, p. 491.
Martin, A.H.M. and Downes, D.: 1972, *Astrophys. Letters* **11**, 219.
Maxwell, A. and Taylor, J.H.: 1968, *Astrophys. Letters* **2**, 191.
Neugebauer, G., Becklin, E.E., Matthews, K. and Wynn-Williams, C.G.: 1978, *Astrophys. J.* **220**, 149.
Pankonin, V. and Downes, D.: 1976, *Astron. Astrophys.* **47**, 303.
Pauliny-Toth, I.I.K., Witzel, A., Preuss, E., Baldwin, J.E. and Hills, R.E.: 1978, *Astron. Astrophys.* (in press).
Pauls, T.A., Mezger, P.G. and Churchwell, E.: 1974, *Astron. Astrophys.* **34**, 327.
Pauls, T. and Mezger, P.G.: 1975, *Astron. Astrophys.* **44**, 259.
Pauls, T., Downes, D., Mezger, P.G. and Churchwell, E.: 1976, *Astron. Astrophys.* **46**, 407.
Reifenstein, E.C., Wilson, T.L., Burke, B.F., Mezger, P.G. and Altenhoff, W.J.: 1970, *Astron. Astrophys.* **4**, 357.
Rieke, G.H., Harper, D.A., Low, F.J. and Armstrong, K.R.: 1973, *Astrophys. J.* **183**, L67.
Rieke, G.H., Telesco, C.M. and Harper, D.A.: 1978, *Astrophys. J.* **220**, 556.
Righini, G., Simon, M. and Joyce, R.R.: 1976, *Astrophys. J.* **207**, 119.
Robinson, B.J. and McGee, R.X.: 1970, *Austral. J. Phys.* **23**, 405.
Rogstad, D.H., Lockhart, I.A. and Whiteoak, J.B.: 1974, *Astron. Astrophys.* **36**, 253.
Sandqvist, Aa: 1974, *Astron. Astrophys.* **33**, 413.
Schmidt, J.: 1978, Ph. D. Thesis, Bonn University.
Schwarz, U.J.: 1978, *Astron. Astrophys.* (in press).
Scoville, N.Z., Solomon, P.M. and Thaddeus, P.: 1972, *Astrophys. J.* **172**, 335.
Swarup, G., Gopal-Krishna and Sarma, N.V.G.: 1974, in F.J. Kerr and S.C. Simonson (eds.), Galactic Radio Astronomy, *IAU Symp. no. 60*, D. Reidel, Dordrecht, p. 499.
Taylor, J.H.: 1968, Ph. D. Thesis, Harvard University.
Thompson, A.R., Riddle, A.C. and Lang, K.R.: 1969, *Astrophys. Letters* **3**, 49.
Thum, C., Mezger, P.G., Pankonin, V. and Schraml, J.: 1978, *Astron. Astrophys.* **64**, L17.
Westbrook, W.E., Werner, M.W., Elias, J.H., Gezari, D.Y., Hauser, M.G., Lo, K.Y. and Neugebauer, G.: 1976, *Astrophys. J.* **209**, 94.
Whiteoak, J.B. and Gardner, F.F.: 1973, *Astrophys. Letters* **13**, 205.
Whiteoak, J.B. and Gardner, F.F.: 1974, *Astron. Astrophys.* **37**, 389.
Willner, S.P.: 1978, *Astrophys. J.* **219**, 870.
Wollman, E.R., Geballe, T.R., Lacy, J.H., Townes, C.H. and Rank, D.M.: 1976, *Astrophys. J. Letters* **205**, L5.
Wollman, E.R., Geballe, T.R., Lacy, J.H., Townes, C.H. and Rank, D.M.: 1977, *Astrophys. J.* **218**, L103.
Wouterloot, J.G.A.: 1978, *Astron. Astrophys.* in preparation.

D. Downes
Max-Planck-Institut für Radioastronomie
Auf dem Hügel 69
D–5300 Bonn 1 (Federal Republic of Germany)

W.M. Goss
U.J. Schwarz
Kapteyn Astronomical Institute
University of Groningen
Groningen (The Netherlands)

J.G.A. Wouterloot
Sterrewacht
Huygens Laboratorium
Wassenaarseweg 78
2405 Leiden (The Netherlands)

Table 1 Parameters of Compact Continuum Sources

(1)	(2) (3)	(4)	(5)	(6) (7)	(8)	(9)	(10)	(11)	(12)	(13)
		Compact Components		(Westerbork data)	Extended Components		(Bonn data)			
No.	Long. Lat.	R.A.(1950)	Dec(1950)	5 GHz flux / Diam. in R.A.	R.A.(1950)	Dec(1950)	Flux density 5 GHz	10.7 GHz	Diam. (arc	Remarks
	(deg.)	(h m s)	(o ' ")	(Jy) (arc sec)	(h m s)	(o ' ")	(Jy)	(Jy)	min)	
1	359.438-0.082	17 41 24.3	-29 26 15	1.3 core 26 1.2 halo	17 41 24.6	-29 26 50	9.9	4.2 5.0	1.3 3x5	core halo
2	359.645-0.056	17 41 48.3	-29 14 53	0.08 10	17 41 49.3	-29 15 24	3.0	1.5	2.0	
3	359.653-0.068	17 41 52.2	-29 14 53	0.06 9						
4	359.716-0.036	17 41 53.9	-29 10 37	0.21 22	17 41 55.7	-29 10 43	11.	-	5.5	
5	359.727-0.034	17 41 55.0	-29 10 00	0.12 14						
6	359.865-0.087	17 42 27.3	-29 04 39	0.09 4	-	-	-	-	-	
7	359.871+0.178	17 41 26.4	-28 55 58	0.05 <4	-	-	-	-	-	
8	359.898-0.066	17 42 27.4	-29 02 18	0.10 <4	-	-	-	-	-	
9[a]	359.930-0.043	17 42 26.5	-28 59 55	- <1	-	-	-	transient radio source		
10[b]	359.945-0.047	17 42 29.5	-28 59 19	26. 45	-	-	-	-	-	Sgr A West
11[c]	359.945-0.046	17 42 29.291	-28 59 17.6	0.2 core 0.001 0.6 halo 0.017	17 42 29.5	-28 59 33	200.	120.	3.7	point source
12[b]	359.962-0.064	17 42 36.	-28 59 00	170. 140.	-	-	-	-	-	Sgr A East
13	359.978-0.077	17 42 41.3	-28 58 33	0.44 6	-	-	-	-	-	
14	359.983+0.027	17 42 18.0	-28 55 02	0.20 <4	17 42 20.4	-28 55 06	-	12.	2.0	
15	0.040+0.019	17 42 27.9	-28 52 21	0.35 11	17 42 26.2	-28 50 21	-	3.7	0.9	
16	0.064-0.307	17 43 47.5	-29 01 22	0.01 <4	-	-	-	-	-	
17	0.078-0.093	17 42 59.4	-28 53 58	0.03 <4	-	-	-	-	-	
18	0.096-0.052	17 42 52.5	-28 51 44	0.03 <4	-	-	-	-	-	
19	0.097-0.165	17 43 19.2	-28 55 15	0.05 <4	-	-	-	-	-	
20	0.098+0.023	17 42 35.5	-28 49 17	0.22 11	17 42 36.8	-28 49 54	-	1.4	<0.7	
21	0.099-0.168	17 43 20.1	-28 55 14	0.02 <4	-	-	-	-	-	
22	0.104+0.074	17 42 24.3	-28 47 21	0.14 <4	17 42 22.6	-28 47 06	-	5.3	1x5	
23	0.119-0.061	17 42 57.9	-28 50 51	0.12 15	-	-	-	-	-	
24	0.120+0.043	17 42 33.9	-28 47 34	0.25 12	-	-	-	-	-	
25	0.135-0.041	17 42 55.6	-28 49 26	0.35 20	-	-	-	-	-	
26	0.160-0.195	17 43 35.2	-28 52 59	0.20 20	-	-	-	-	-	
27	0.160-0.061	17 43 03.9	-28 48 47	0.04 <4	-	-	-	-	-	
28	0.160-0.047	17 43 00.5	-28 48 19	0.08 7	-	-	-	-	-	
29	0.162-0.064	17 43 04.7	-28 48 46	0.34 20						
30	0.174-0.182	17 43 34.2	-28 51 51	0.53 22	17 43 25.3	-28 51 19	-	16.	1.3x7	
31	0.175-0.080	17 43 10.5	-28 48 35	0.18 14	-	-	-	-	-	
32	0.182-0.039	17 43 01.9	-28 46 55	0.08 8	-	-	-	-	-	
33	0.187-0.055	17 43 06.4	-28 47 12	0.05 5	-	-	-	-	-	
34	0.191-0.133	17 43 25.0	-28 49 26	0.02 <4	-	-	-	-	-	
35	0.195-0.068	17 43 10.5	-28 47 10	0.08 <4	-	-	-	-	-	
36	0.196-0.406	17 44 29.7	-28 57 46	0.01 <4	-	-	-	-	-	
37	0.196-0.099	17 43 17.9	-28 48 08	0.13 15	-	-	-	-	-	
38	0.196-0.059	17 43 08.7	-28 46 51	0.07 5	-	-	-	-	-	
39	0.197-0.107	17 43 19.8	-28 48 18	0.04 8	-	-	-	-	-	
40	0.198-0.034	17 43 02.9	-28 45 58	0.08 11	-	-	-	-	-	
41	0.206-0.127	17 43 25.8	-28 48 30	0.20 20	-	-	-	-	-	
42	0.208-0.002	17 42 57.0	-28 44 26	0.15 <4	-	-	-	-	-	
43	0.217-0.085	17 43 17.6	-28 46 34	0.26 20	17 43 17.6	-28 47 06	-	0.5	≤1.0	
44	0.218-0.151	17 43 33.3	-28 48 37	0.14 20	-	-	-	-	-	
45	0.333-0.012	17 43 17.3	-28 38 22	0.40 26	-	-	-	-	-	
46	0.346-0.027	17 43 22.6	-28 38 11	0.05 <4	-	-	-	-	-	
47	0.382+0.017	17 43 17.6	-28 34 58	1.23 27	17 43 16.3	-28 35 17	2.	-	-	
48	0.467-0.639	17 46 02.8	-28 51 12	0.25 30	-	-	-	-	-	
49	0.472-0.054	17 43 46.8	-28 32 36	0.55 13	-	-	-	-	-	
50	0.485-0.664	17 46 11.1	-28 51 00	0.32 45	17 46 12.7	-28 50 56	2.6	-	2.2	double source
51	0.485-0.058	17 43 49.8	-28 32 05	0.22 9	17 44 00.3	-28 30 28		2.4	1.1	
52	0.490-0.074	17 43 54.0	-28 32 19	0.35 12	17 43 50	-28 31 31	25.	2.9	0.9	
53	0.493-0.051	17 43 49.2	-28 31 25	0.90 19	17 43 50.7	-28 30 22		3.4	1.4	
54	0.523-0.042	17 43 51.5	-28 29 37	0.24 11	17 43 52	-28 30 35		11.	3.5	
55	0.542-0.662	17 46 18.8	-28 48 02	0.54 58						
56[d]	0.547-0.851	17 47 03.7	-28 53 39	0.36[d] <15	17 47 05.6	-28 52 53	2.9	-	2.3	near H_2O maser
57	0.577-0.635	17 46 17.6	-28 45 22	0.21[d] 32	17 46 15.2	-28 45 25	4.7	-	3.2	
58[d]	0.586-0.869	17 47 13.5	-28 52 11	0.69[d] 25	-	-	-	-	-	
59	0.598-0.049	17 44 03.8	-28 26 01	0.45 8	17 44 04.6	-28 25 55	-	2.1	≤0.6	MD2
60	0.601-0.051	17 44 04.8	-28 25 54	0.8 <5						
61	0.602-0.620	17 46 17.6	-28 43 37	0.12 30	-	-	-	-	-	
62	0.629-0.028	17 44 03.3	-28 23 45	1.4 11	17 44 04.1	-28 24 00	-	1.1	≤0.6	MD1
63	0.657-0.007	17 44 02.4	-28 21 41	0.6 8	-	-	-	-	-	
64	0.658-0.014	17 44 04.3	-28 21 50	0.8 12	-	-	-	-	-	
65	0.666-0.031	17 44 09.3	-28 21 57	2.8 14	17 44 11.6	-28 24 25	-	3.3	≤0.6	MD3
66	0.667-0.037	17 44 10.7	-28 22 05	4.9 7						MD5
67	0.670-0.045	17 44 13.1	-28 22 12	0.5 10	17 44 10.7 17 44 12.0	-28 21 37 -28 21 47	54.	20. 30.	0.8 3.5	
68	0.679-0.028	17 44 10.5	-28 21 12	6.0 11	-	-	-	-	-	MD4
69	0.687-0.034	17 44 12.9	-28 20 57	1.5 6	-	-	-	-	-	MD6
70	0.692-0.046	17 44 16.3	-28 21 06	0.9 9	-	-	-	-	-	MD7
71	0.835+0.186	17 43 43.1	-28 06 29	0.25 16	17 43 40.7	-28 06 27	1.4	1.2	1.1	
72	0.863+0.087	17 44 09.9	-28 08 12	0.45 30	17 44 10.9	-28 08 09	8.6	3.2 core 5.8 halo	1.3 4.5	non-thermal
73	0.873+0.087	17 44 11.4	-28 07 42	0.85 45						
74	1.127-0.106	17 45 32.2	-28 00 42	1.07 11	17 45 31.5 17 45 29.	-28 00 45 -28 00 00	15.3	2.5 8.2	1.1 5.0	
					17 45 31.5	-28 05 48	7.5	-	4.3	non-thermal
					17 45 27.5	-27 58 12	-	0.3	≤0.9	
					17 45 42	-27 54 00	2.	2.	3.	

a) Transient radio source; data at 0.96 GHz from Davies et al. (1976a); possibly identified with transient X-ray source A1742-28 (Eyles et al. 1975).

b) Sgr A West and East; data from Ekers et al. (1975).

c) Radio point source; data at 7.8 GHz from Kellermann et al. (1977); see also Brown et al. (1978).

d) Data at 1.4 GHz from Miley (private communication).

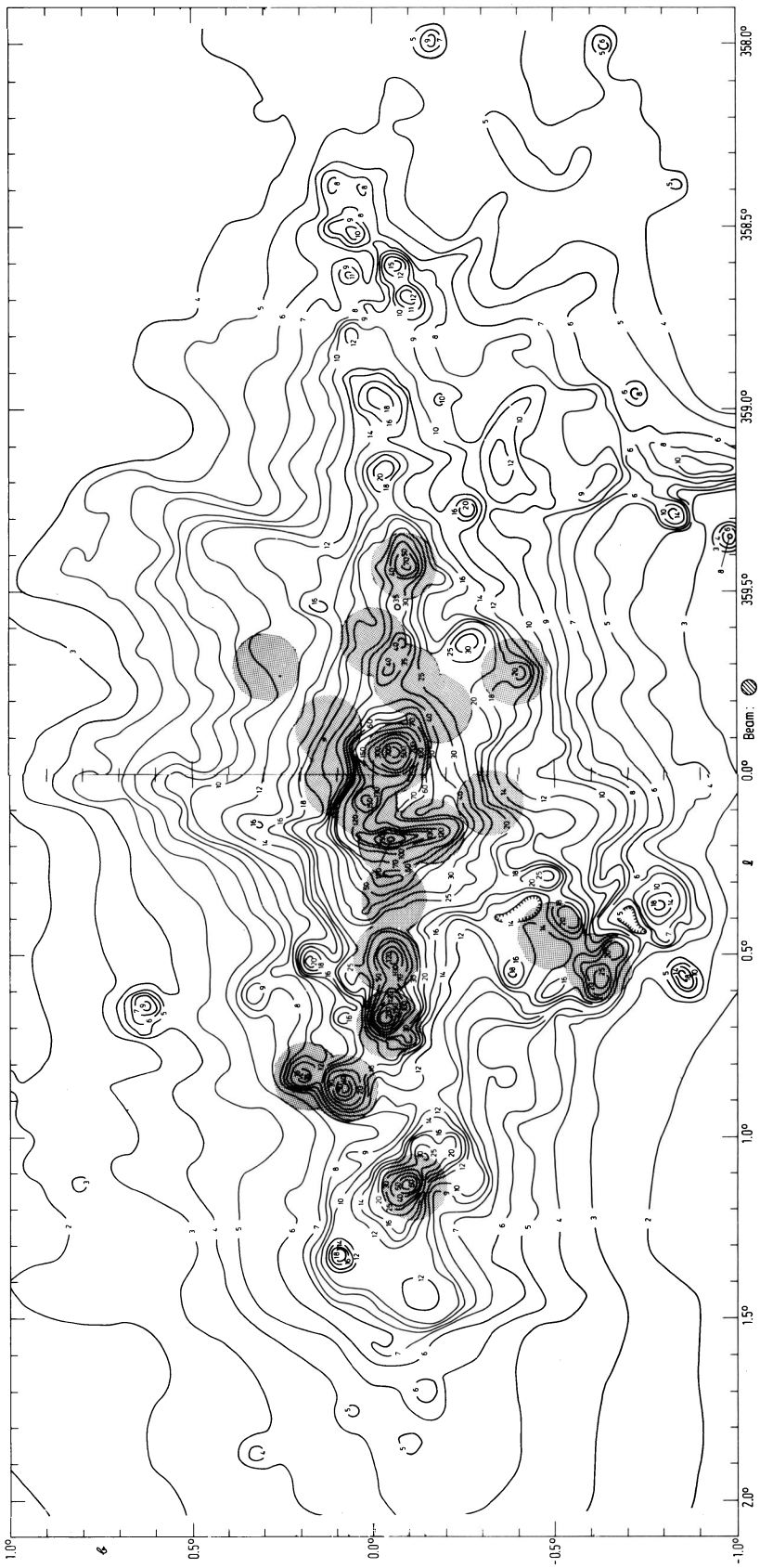

Figure 1 Fields which have been searched at Westerbork for compact components at 5 GHz (shaded circles), superimposed on the map of radio continuum emission at 4.875 GHz made with a 2.6′ beam with the 100-m telescope (Altenhoff *et al.* 1978). The contour unit at 4.875 GHz is 0.1 Jy for an equivalent point source $=0.13$ K $T_a=0.20$ K T_b. The diameter of the shaded circles is 10.8′, the half-power width of the Westerbork primary beam at 5 GHz.

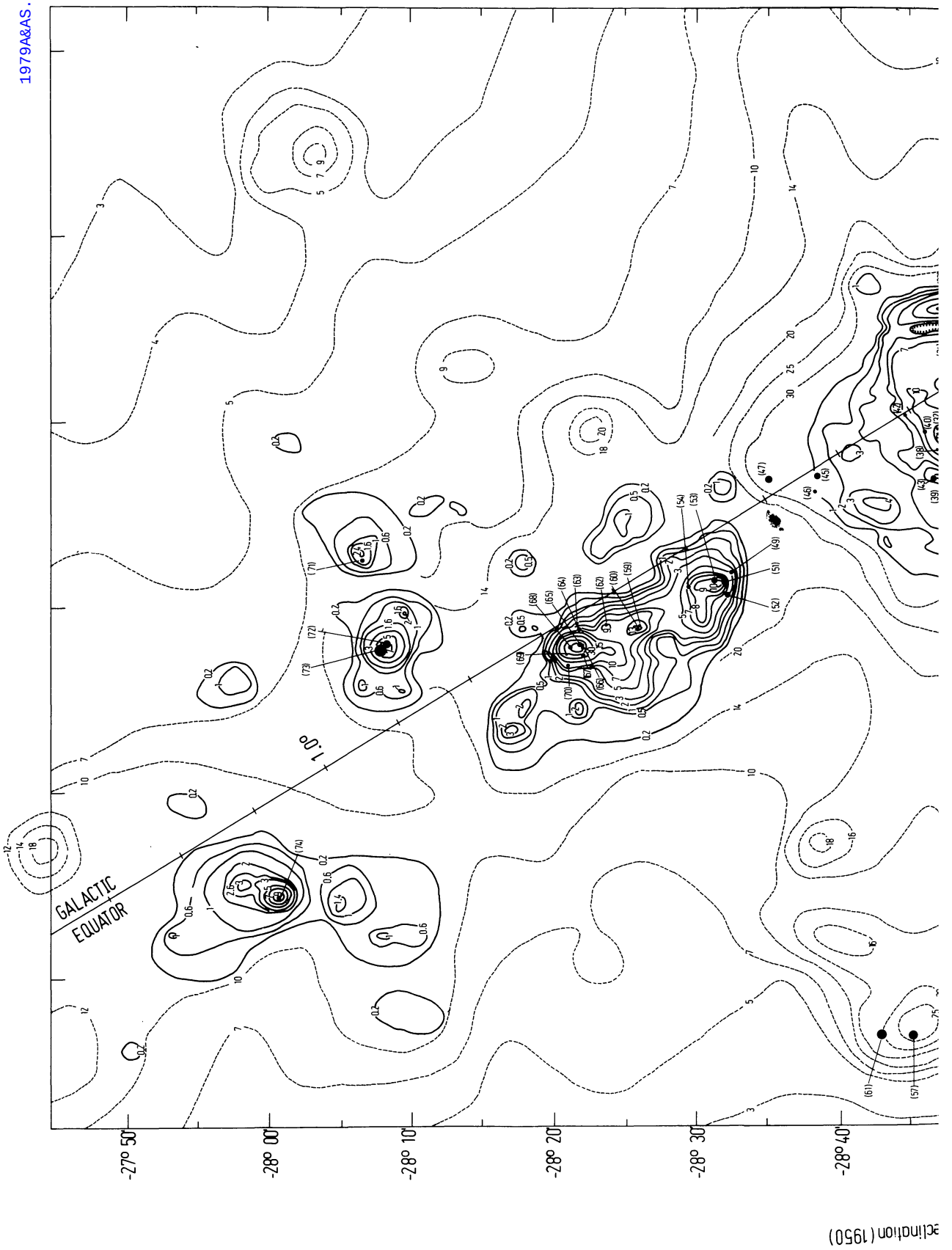

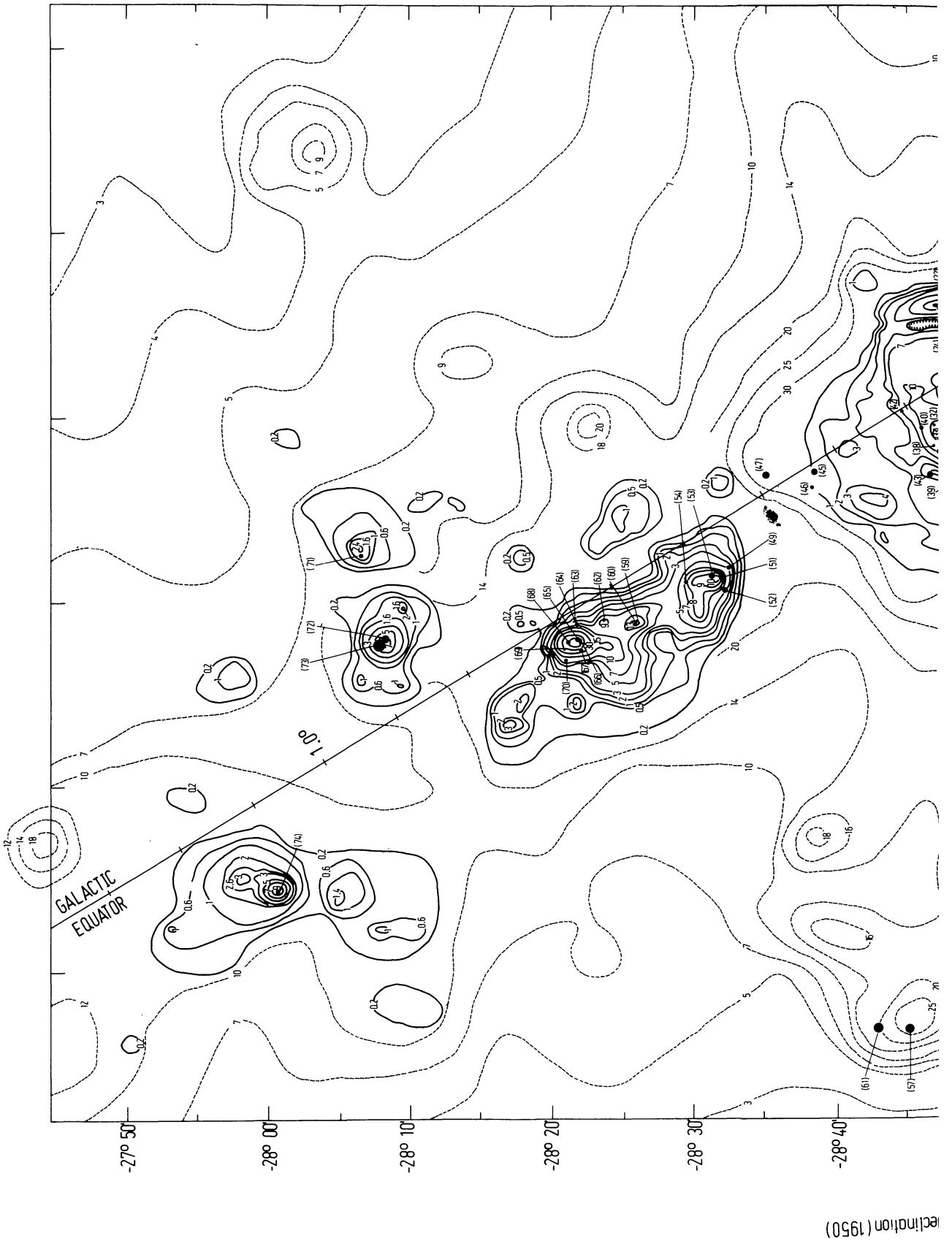

1979A&AS...35....1D

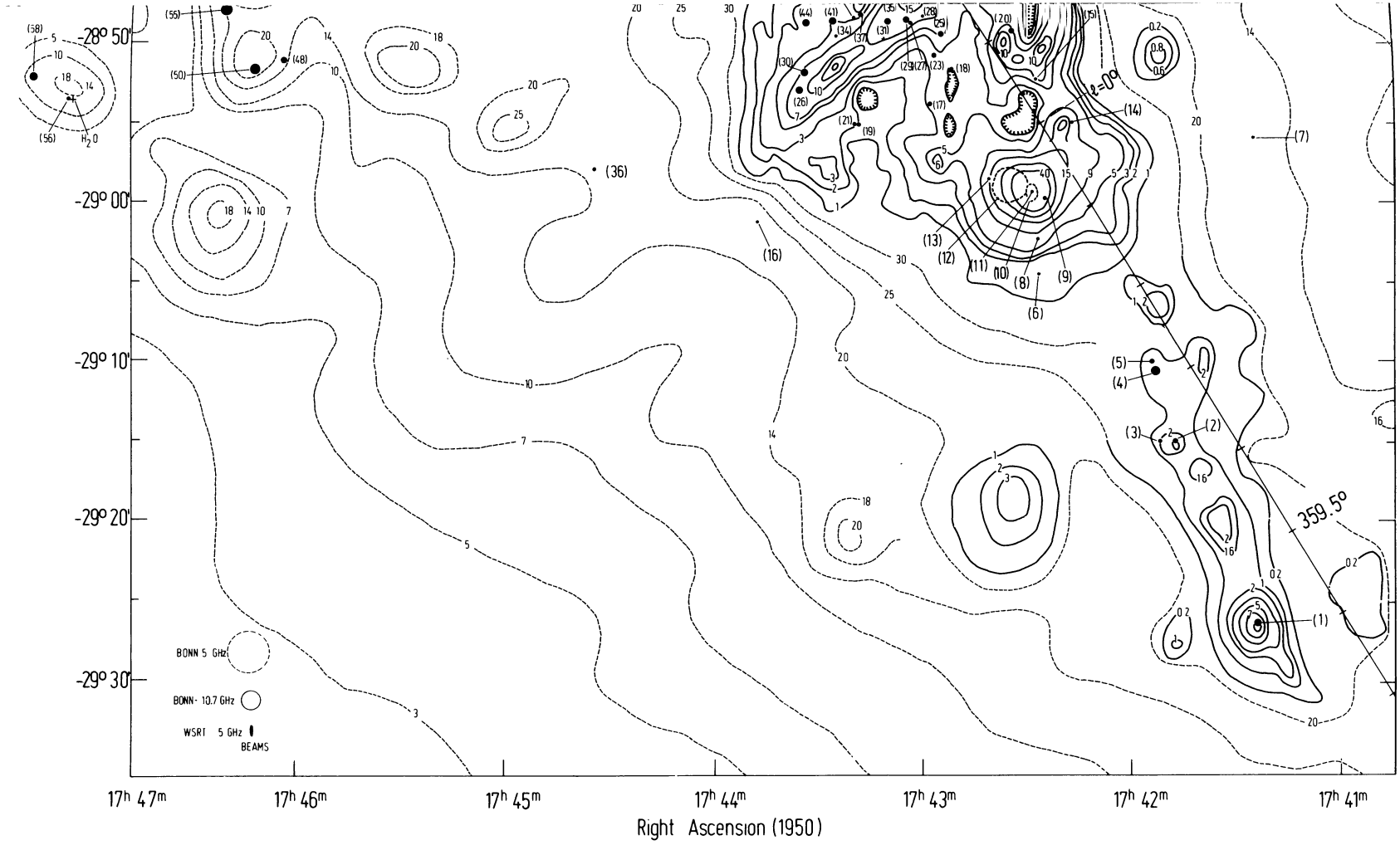

Figure 2 Composite diagram of radio continuum sources in the galactic center region. Dashed contours =4.875 GHz data from Altenhoff *et al.* (1978), beam =2.6′, contour unit =0.1 Jy/beam area. Solid-line contours =10.7 GHz data from the 100-m telescope, beam =1.3′, contour unit =0.283 K T_a=0.47 K main-beam T_b=0.27 Jy/beam area. Black dots=compact components detected at Westerbork. The diameter of the dots is equal to the diameter of the compact sources in R.A. Numbers in parentheses next to the black dots are the identification numbers given in the source list. The half-power diameters of Sgr A East and West are indicated by dashed circles.

1979A&AS...35....1D

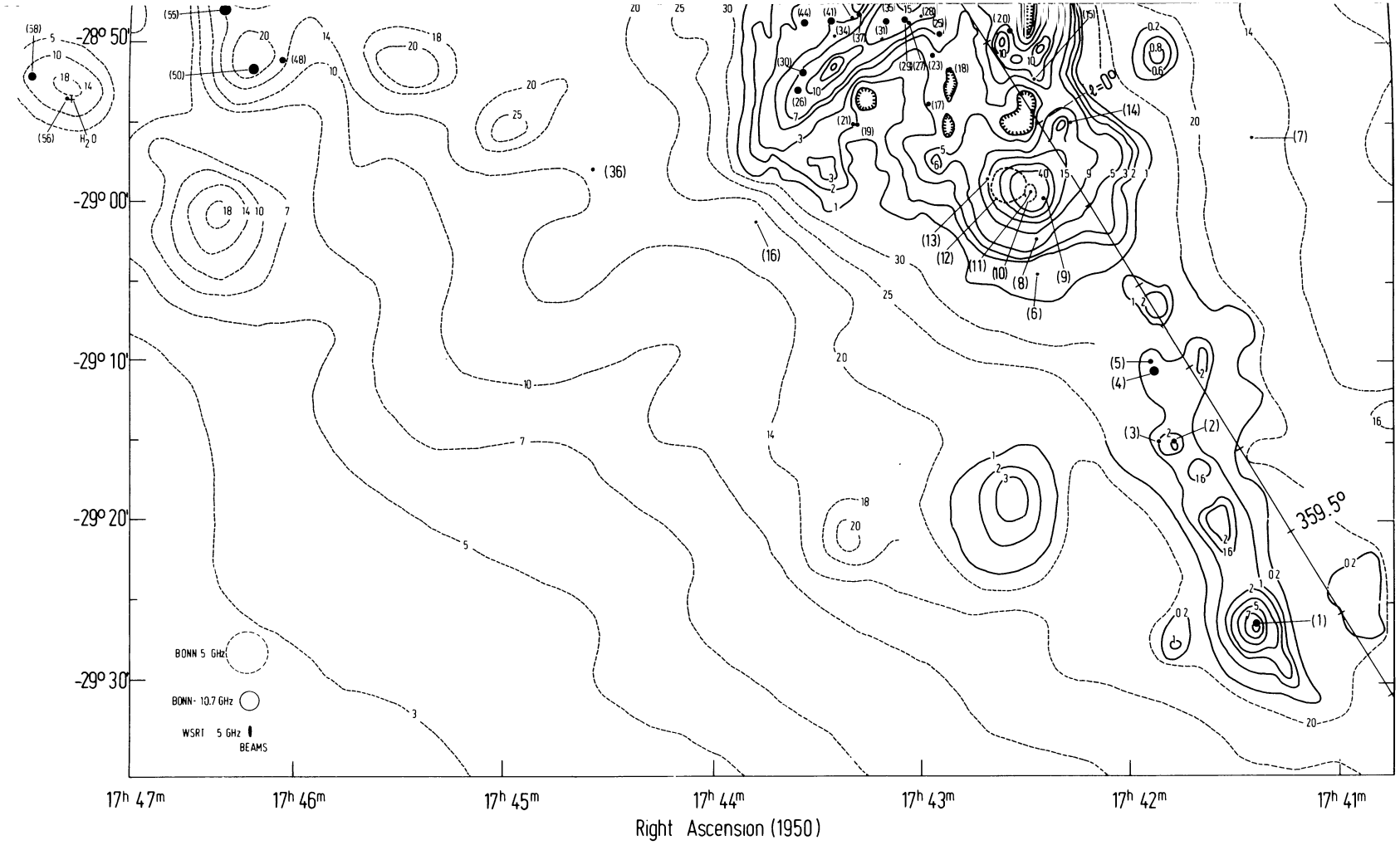

Figure 2 Composite diagram of radio continuum sources in the galactic center region. Dashed contours =4.875 GHz data from Altenhoff *et al.* (1978), beam =2.6′, contour unit =0.1 Jy/beam area. Solid-line contours =10.7 GHz data from the 100-m telescope, beam =1.3′, contour unit =0.283 K T_a=0.47 K main-beam T_b=0.27 Jy/beam area. Black dots=compact components detected at Westerbork. The diameter of the dots is equal to the diameter of the compact sources in R.A. Numbers in parentheses next to the black dots are the identification numbers given in the source list. The half-power diameters of Sgr A East and West are indicated by dashed circles.

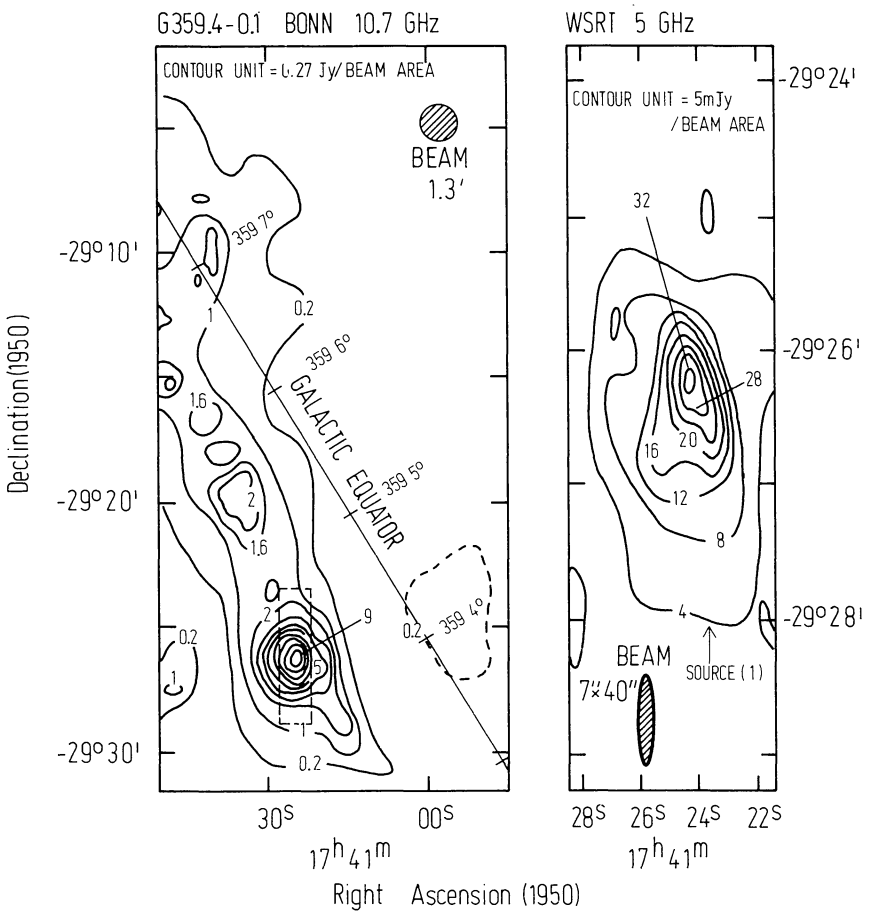

Figure 3 Maps of the source G359.4–0.1, made with the 100-m telescope at 10.7 GHz (left) and with the Westerbork telescope at 5 GHz (right). The compact source is number (1) in the source list. The dashed rectangle on the Bonn map shows the area covered by the Westerbork diagram.

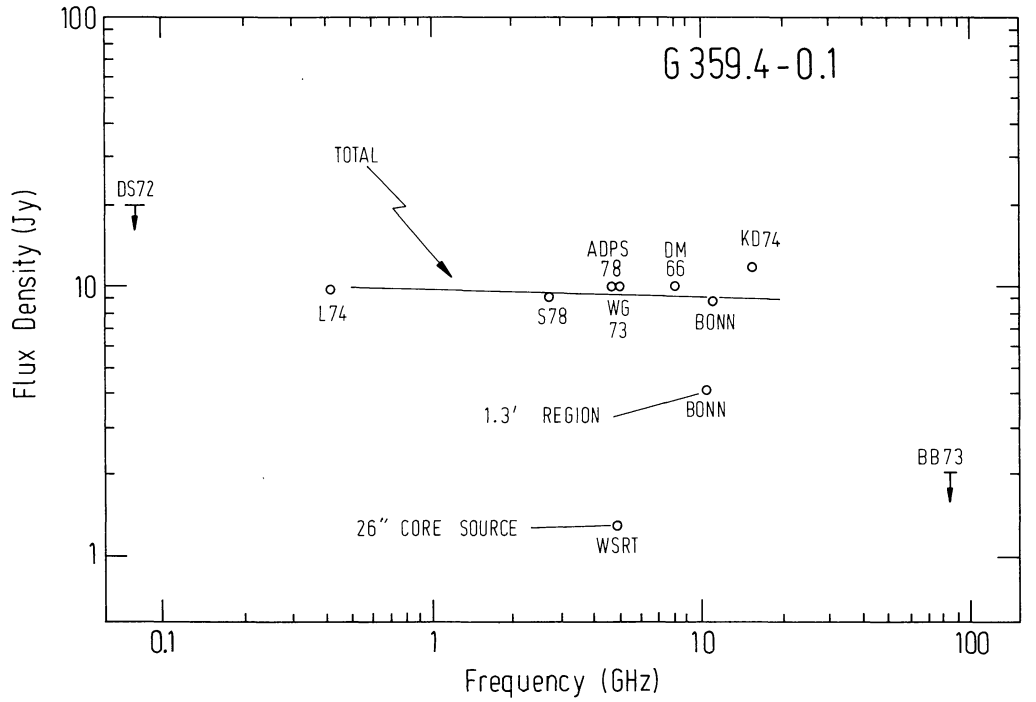

Figure 4 Spectrum of G359.4–0.1, derived from observations with beamwidths <5'. The data points are identified by author's initials and year of publication. Some of the published results have been revised in accordance with the source model given in the text. Points labelled "Bonn" and "WSRT" are from this paper.

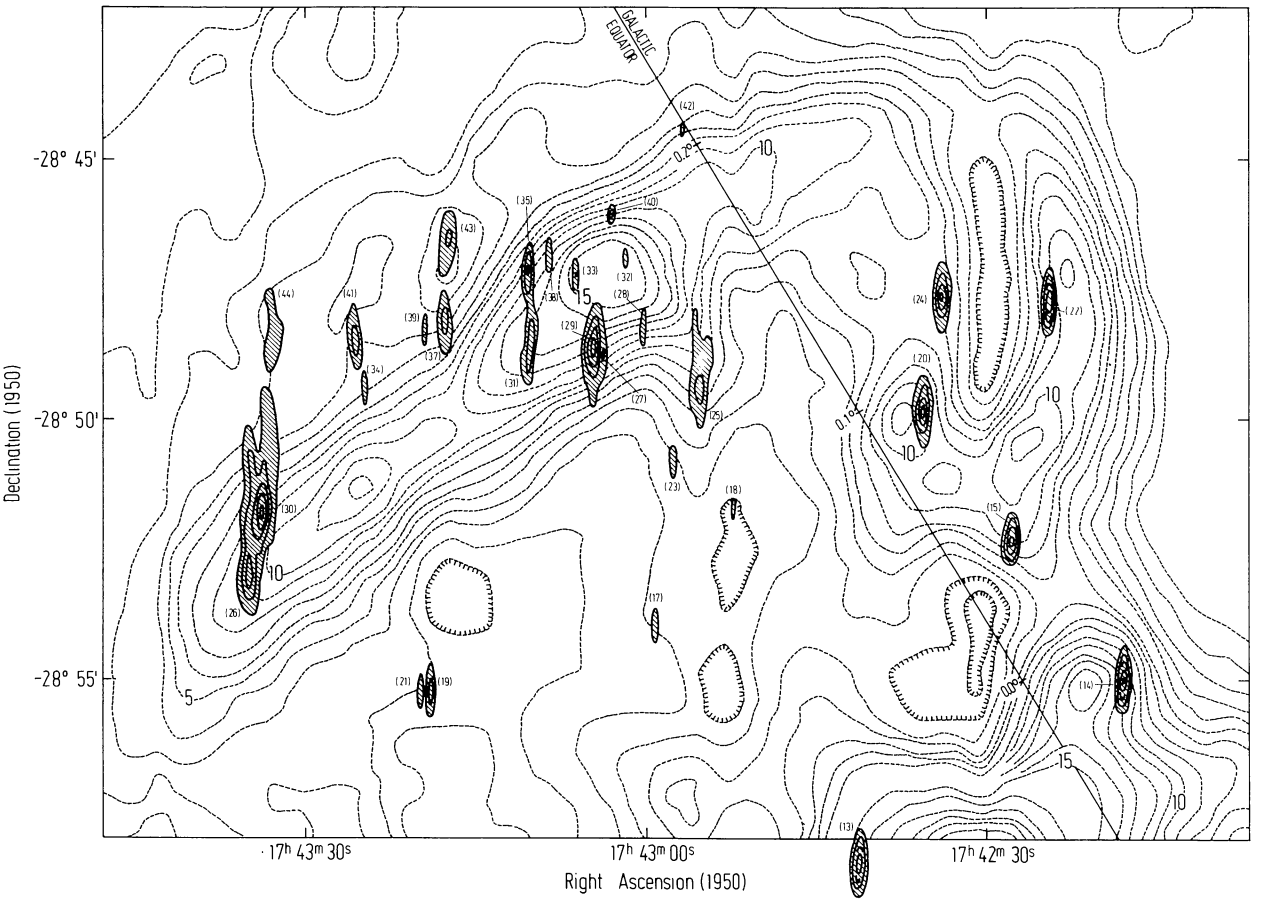

Figure 5 Solid contours, with shading, denote the compact sources found at Westerbork in the region $\ell = 0.0°$ to 0.2°, near the galactic equator. Solid contours are in steps of 10 mJy/beam area, uncorrected for the attenuation by the primary beam pattern. The restored beam was $6'' \times 36''$. Dashed contours are from the Bonn 10.7 GHz map, with half-power beamwidth 1.3′ and contour unit 0.27 Jy/beam area. Numbers in parantheses next to the compact components are the identification numbers in the source list.

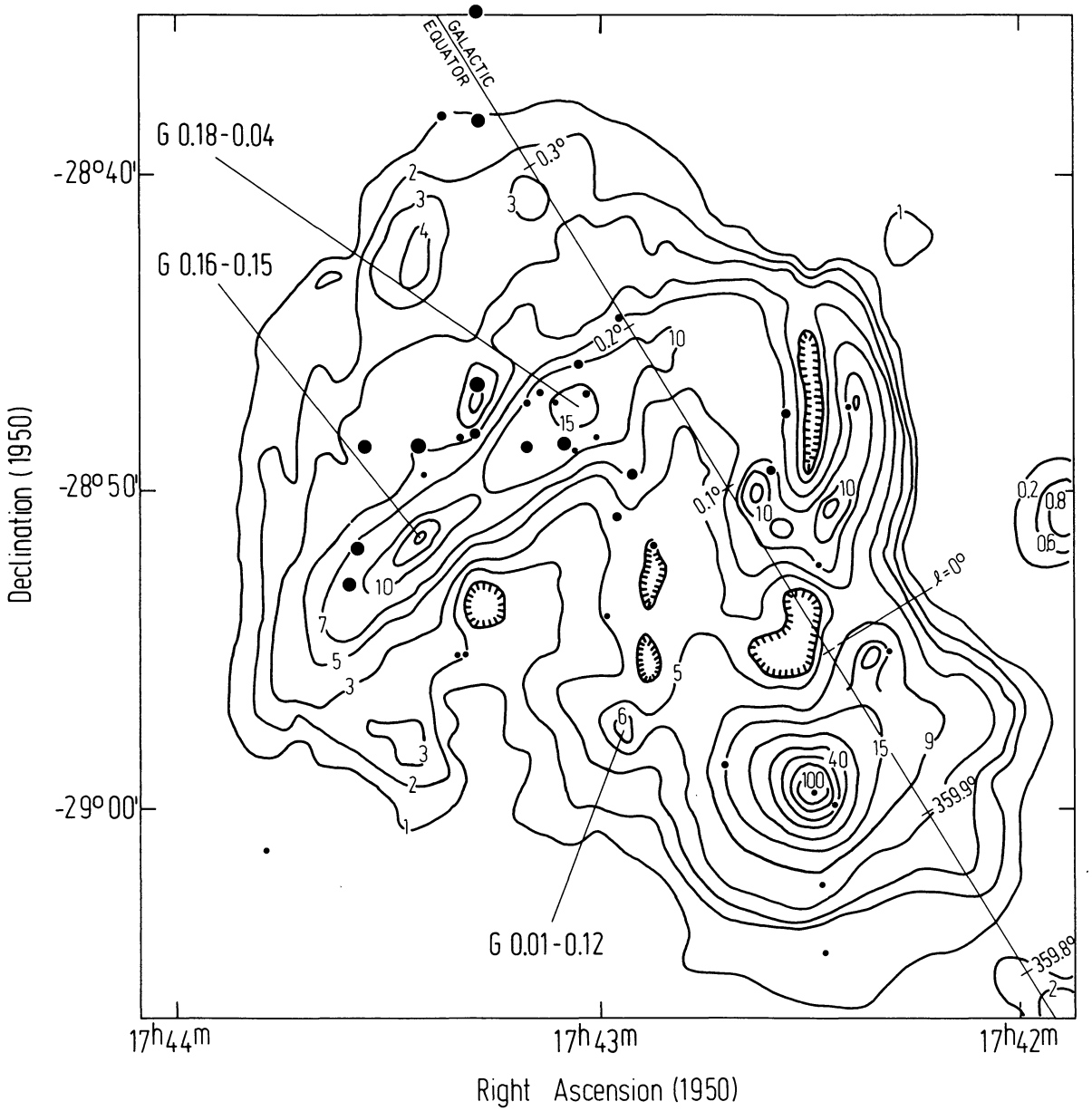

Figure 6 Expanded view of the field in figure 5, with the compact sources found at Westerbork (black dots) superimposed on the Bonn map at 10.7 GHz. The diameters of the dots are equal to the deconvolved half-widths of the sources in R.A.

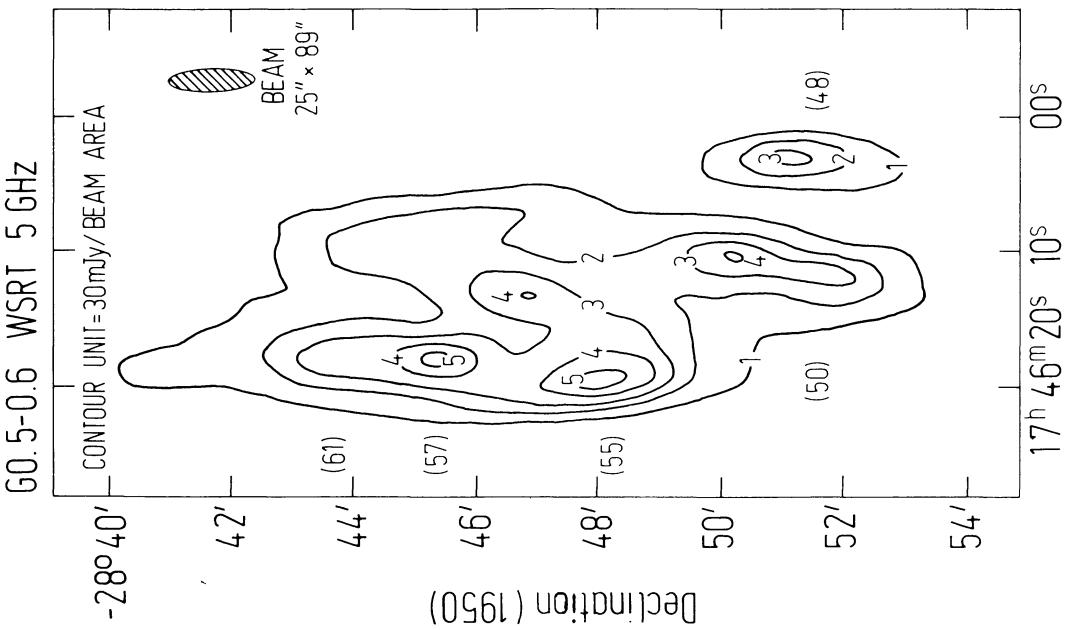

Figure 8 Cleaned map of the source complex G0.5–0.6 made from Westerbork data at 5 GHz. Identification numbers from the source list are given in parentheses.

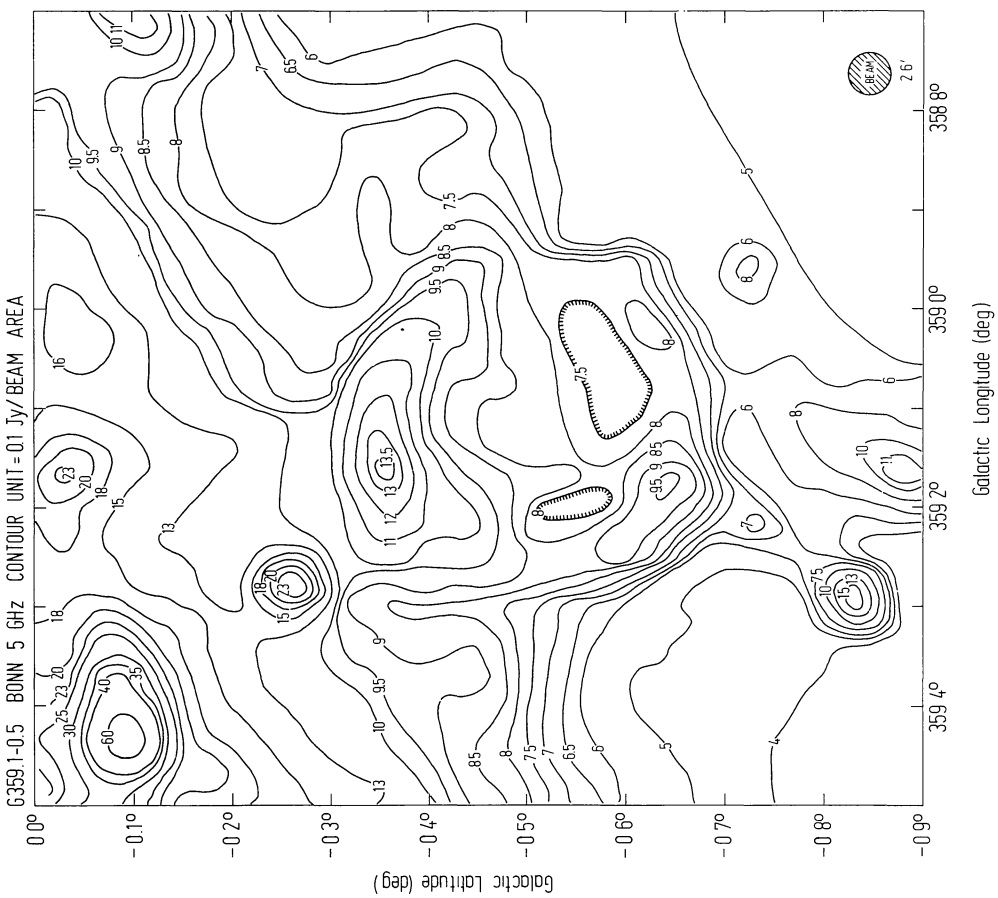

Figure 7 Map of G359.1–0.5, a previously unrecognized shell source, possibly a supernova remnant, from the galactic survey data of Altenhoff *et al.* (1978).

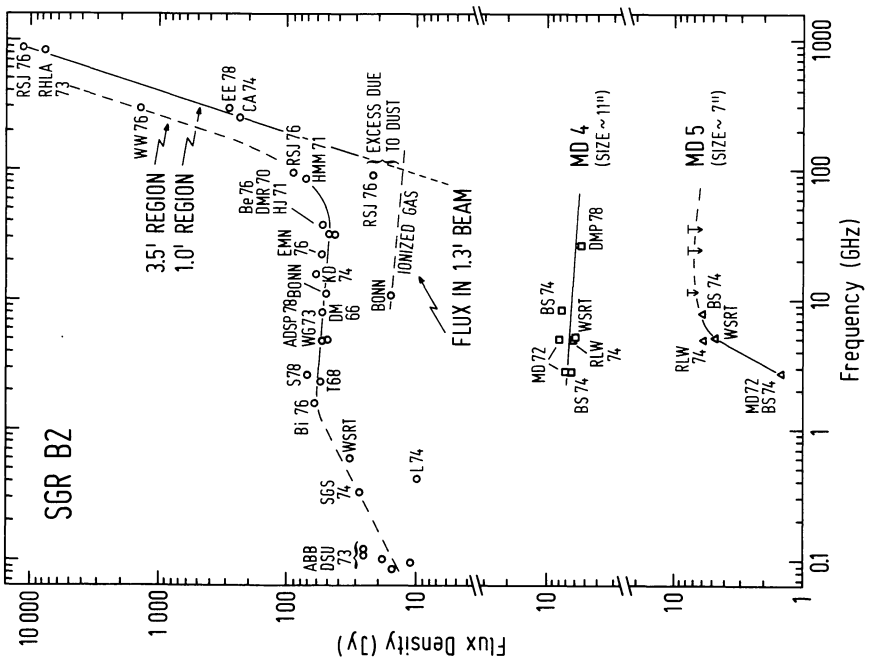

Figure 10 Spectra of components in Sgr B2. Labels are as in figure 4. We have re-derived some of the flux densities from data in the original publications. The uppermost radio curve corresponds to the total flux density of Sgr B2, as measured with single-dish telescopes with beamwidths $<5'$.

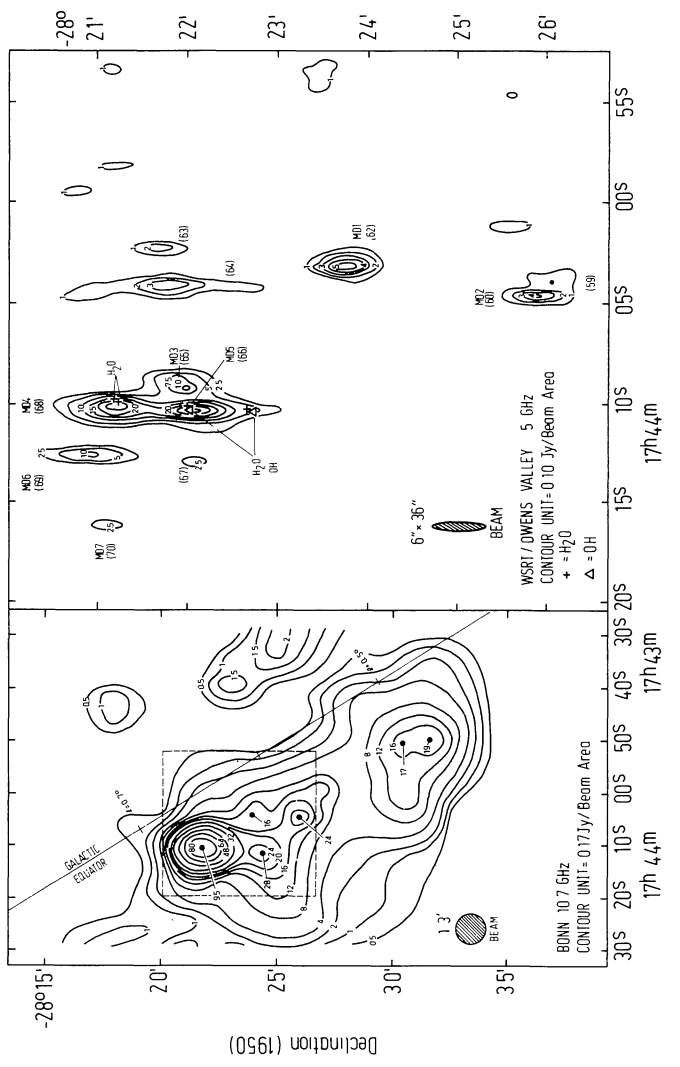

Figure 9 (Left): Bonn map of Sgr B2 at 10.7 GHz. The dashed rectangle indicates the area of the diagram at right. (Right): Cleaned map of Sgr B2 at 5 GHz, from a combination of data from Westerbork (this paper) and from Owens Valley (Rogstad *et al.* 1974). Identification numbers from the source list are given in parentheses, along with designations in the list of Martin and Downes (1972). Positions of H_2O masers (crosses) are from Genzel *et al.* (1976) and Forster *et al.* (1978). Positions of OH masers (triangles) are from Goss *et al.* (1976) and Bieging (1976).

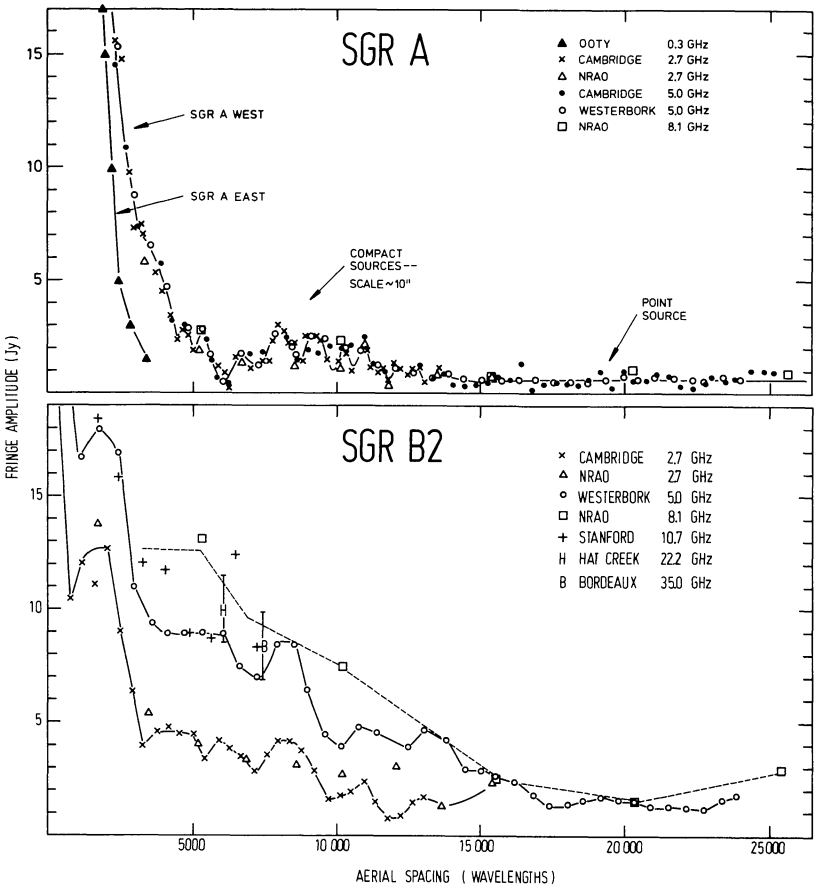

Figure 11 Fringe amplitude vs. spacing of Sgr A and Sgr B2 measured with the following interferometers: Ooty (Bagri 1975), Cambridge (Downes and Martin 1971, Martin and Downes 1972), NRAO (Balick and Sanders 1974), Westerbork (Ekers *et al.* 1975, and this paper), Stanford (Felli *et al.* 1974), Hat Creek and Bordeaux (A. Baudry, private communication). Most of the observations were made close to transit, except for the Ooty data, which are an average of measurements at baseline position angles of 310° and 340°.

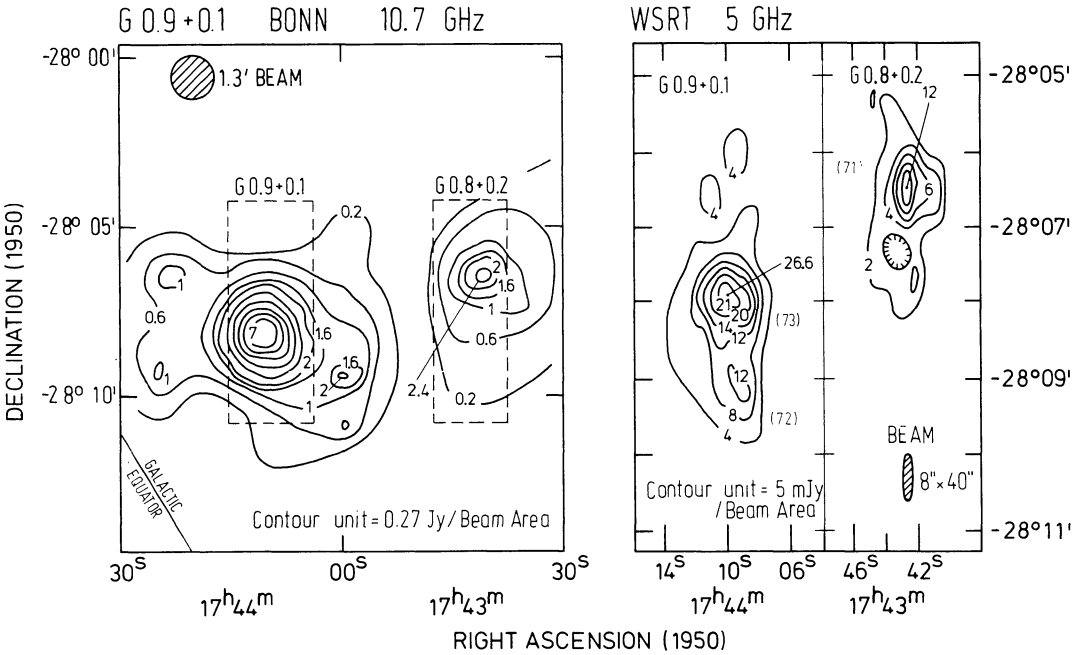

Figure 12 (Left): Bonn map of G0.9+0.1 and G0.8+0.2 at 10.7 GHz. The regions in the dashed rectangles are shown in the maps at the right.

(Right): Cleaned Westerbork maps at 5 GHz. Identification numbers from the source list are in parentheses.

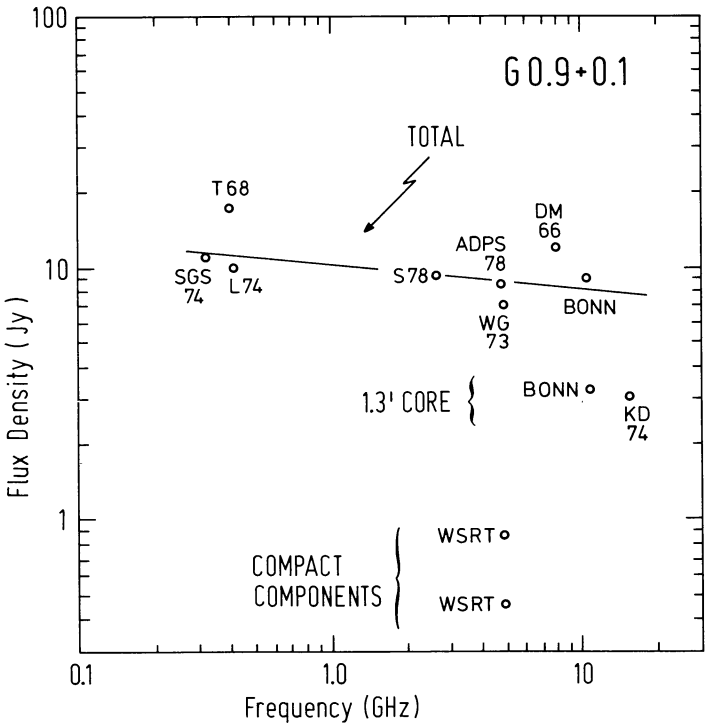

Figure 13 Spectra of G0.9+0.1, from observations with beamwidths $<5'$. Labels are as in figure 4.

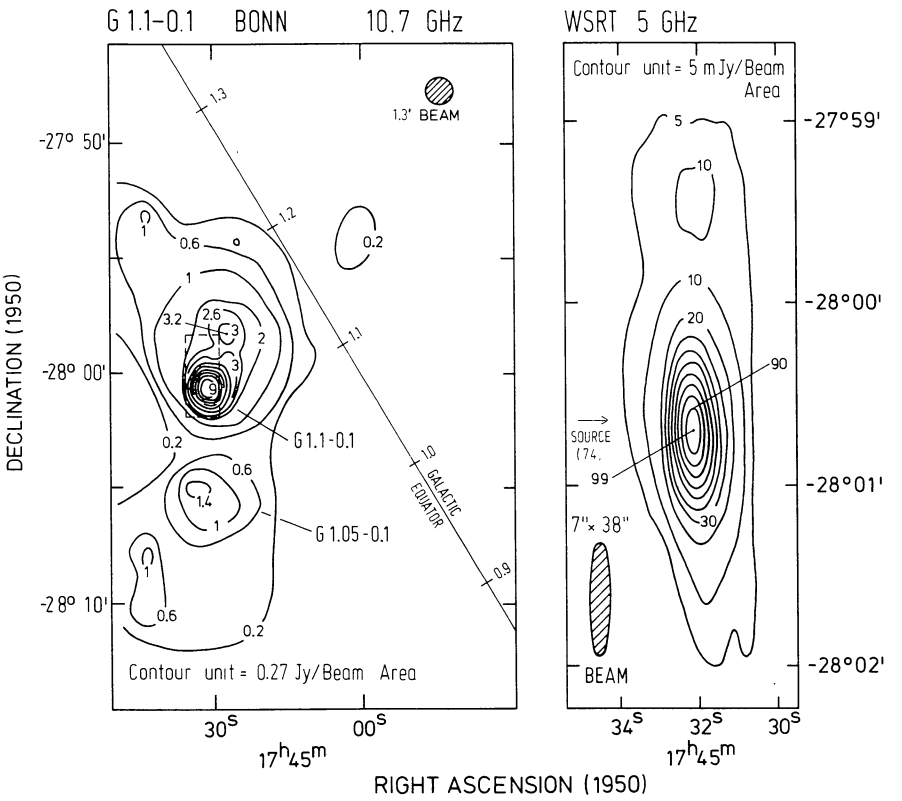

Figure 14 (Left): Bonn map of G1.1–0.1 at 10.7 GHz. The dashed rectangle indicates the area of the diagram at right. (Right): Cleaned map of the dominant compact source observed at Westerbork at 5 GHz.

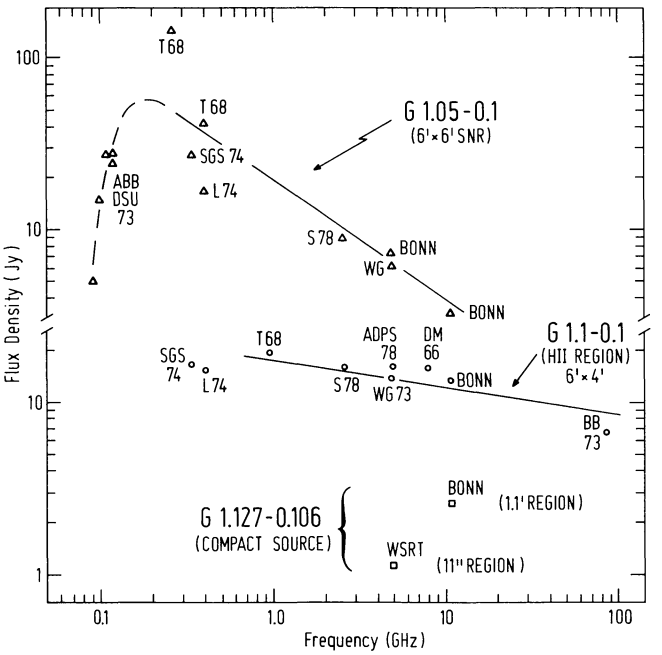

Figure 15 Spectra of the sources in the field near G1.1–0.1, from measurements with beamwidths <5′. Labels are as in figure 4.

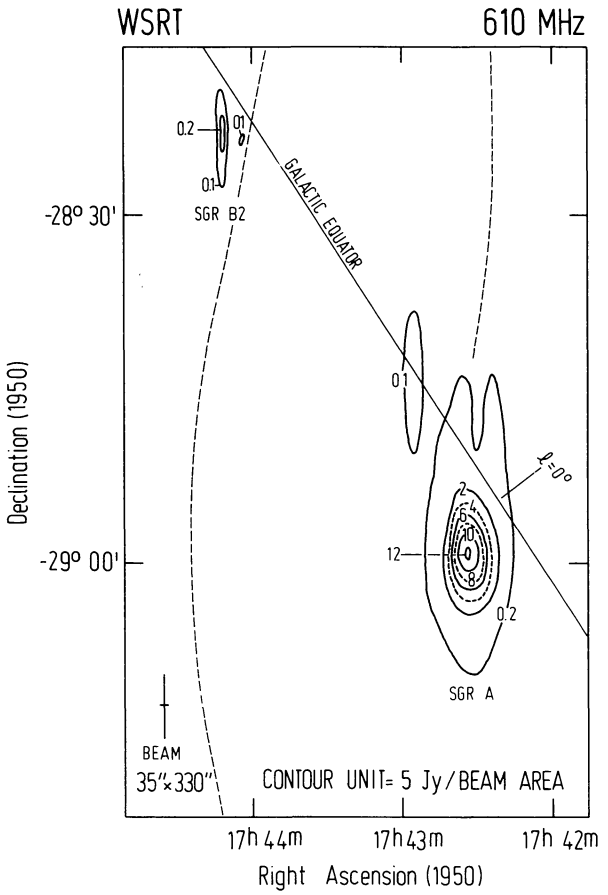

Figure 16 Cleaned map of the region of Sgr A and Sgr B2 made at Westerbork at 610 MHz.